

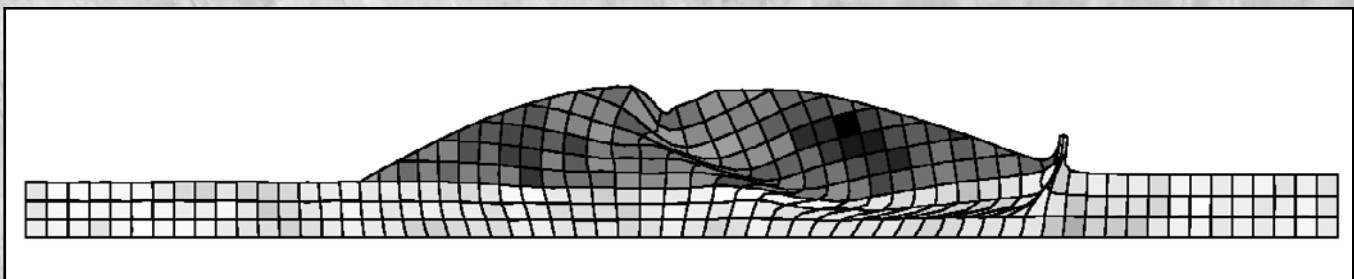
RECLAMATION

Managing Water in the West

Report DSO-09-02

Probabilistic Slope Stability Analysis Using the Random Finite Element Method (RFEM)

Report of Findings



Dam Safety Technology Development Program



U.S. Department of the Interior
Bureau of Reclamation
Technical Service Center
Denver, Colorado

December 2009

REPORT DOCUMENTATION PAGE

*Form Approved
OMB No. 0704-0188*

The public reporting burden for this collection of information is estimated to average 1 hour per response, including the time for reviewing instructions, searching existing data sources, gathering and maintaining the data needed, and completing and reviewing the collection of information. Send comments regarding this burden estimate or any other aspect of this collection of information, including suggestions for reducing the burden, to Department of Defense, Washington Headquarters Services, Directorate for Information Operations and Reports (0704-0188), 1215 Jefferson Davis Highway, Suite 1204, Arlington, VA 22202-4302. Respondents should be aware that notwithstanding any other provision of law, no person shall be subject to any penalty for failing to comply with a collection of information if it does not display a currently valid OMB control number.

PLEASE DO NOT RETURN YOUR FORM TO THE ABOVE ADDRESS.

1. REPORT DATE (DD-MM-YYYY) December 2009		2. REPORT TYPE Final		3. DATES COVERED (From - To)	
4. TITLE AND SUBTITLE Probabilistic Slope Stability Analysis Using the Random Finite Element Method (RFEM)—Report of Findings				5a. CONTRACT NUMBER	
				5b. GRANT NUMBER	
				5c. PROGRAM ELEMENT NUMBER	
6. AUTHOR(S) Giorgia Fulcheri deWolfe, Bureau of Reclamation, 86-68311, Denver CO				5d. PROJECT NUMBER	
				5e. TASK NUMBER	
				5f. WORK UNIT NUMBER	
7. PERFORMING ORGANIZATION NAME(S) AND ADDRESS(ES) Bureau of Reclamation, Technical Service Center, Denver Federal Center, P.O. Box 25007, Denver CO 80225				8. PERFORMING ORGANIZATION REPORT NUMBER DSO-09-02	
9. SPONSORING/MONITORING AGENCY NAME(S) AND ADDRESS(ES) Bureau of Reclamation, Dam Safety Office, Denver Federal Center, P.O. Box 25007, Denver CO 80225				10. SPONSOR/MONITOR'S ACRONYM(S)	
				11. SPONSOR/MONITOR'S REPORT NUMBER(S) DSO-09-02	
12. DISTRIBUTION/AVAILABILITY STATEMENT Available from National Technical Information Service, 5285 Port Royal Road, Springfield VA 22161					
13. SUPPLEMENTARY NOTES					
14. ABSTRACT This research developed a computer program based on the random finite element method (RFEM), able to estimate the probability of failure of slopes while fully accounting for spatial variability controlled through an input parameter called the <i>spatial correlation length</i> . The elasto-plastic finite element slope stability method makes no <i>a priori</i> assumptions about the shape or location of the critical failure mechanism and therefore, offers very significant benefits over traditional limit equilibrium methods in the analysis of highly variable soils. Loadings of particular interest in this project include seismic events and potential instability caused during construction or modification of a dam. The probability of failure can be used to prioritize dam safety activities within a risk context. The risk reduction benefits in terms of money spent per unit reduction in failure probability of risk can provide a useful measure for comparing dam safety modification alternatives.					
15. SUBJECT TERMS random finite element method (RFEM), probabilistic slope stability analysis, spatial correlation length, spatial variability of soil properties, liquefaction, random fields					
16. SECURITY CLASSIFICATION OF:			17. LIMITATION OF ABSTRACT SAR	18. NUMBER OF PAGES 61	19a. NAME OF RESPONSIBLE PERSON Giorgia deWolfe
a. REPORT UL	b. ABSTRACT UL	a. THIS PAGE UL			19b. TELEPHONE NUMBER (Include area code) 303-445-3027

Probabilistic Slope Stability Analysis Using the Random Finite Element Method (RFEM)

Report of Findings

Dam Safety Technology Development Program

prepared by

Giorgia Fulcheri deWolfe



**U.S. Department of the Interior
Bureau of Reclamation
Technical Service Center
Civil Engineering Services Division
Geotechnical Engineering Group 1
Denver, Colorado**

December 2009

On the cover.—Probabilistic slope stability model accounting for spatial variation of soil properties.

Mission Statements

The mission of the Department of the Interior is to protect and provide access to our Nation's natural and cultural heritage and honor our trust responsibilities to Indian Tribes and our commitments to island communities.

The mission of the Bureau of Reclamation is to manage, develop, and protect water and related resources in an environmentally and economically sound manner in the interest of the American public.

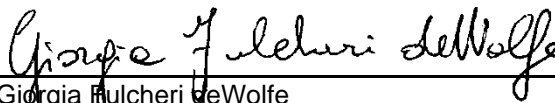
BUREAU OF RECLAMATION
Technical Service Center
Geotechnical Engineering Group 1, 86-68311

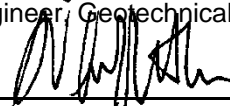
Report DSO-09-02

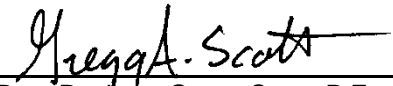
Probabilistic Slope Stability Analysis
Using the Random Finite Element Method
(RFEM)

Report of Findings

Dam Safety Technology Development Program
Denver, Colorado


 Prepared: Georgia Fulcheri deWolfe
 Civil Engineer, Geotechnical Engineering Group 1, 86-68311

 9/16/09
 Checked: Dr. D.V. Griffiths P.E., PhD,
 Professor at Colorado School of Mines

 9/8/2009
 Peer Review: Gregg Scott, P.E.
 Civil Engineer, Geotechnical Engineering Group 2, 86-68312
 Date

REVISIONS					
Date	Description	Prepared	Checked	Technical Approval	Peer Review

Contents

	<i>page</i>
Introduction.....	1
Scope.....	1
Program Description.....	2
Program Methodology and Theory.....	2
Slope stability theory.....	2
Probabilistic random theory.....	7
Input File Description.....	9
Data Output File Description.....	17
Graphical Outputs.....	19
Case History Probabilistic Analysis.....	22
Fruitgrowers Dam.....	22
Background analyses.....	22
Current analyses.....	25
Fruitgrowers deterministic and probabilistic results comparison between the programs <i>Pf-slope</i> and <i>Slope/W</i>	30
Ridgway Dam.....	36
Background analyses.....	40
Current analyses.....	40
Ridgway deterministic and probabilistic results comparison between <i>Pf-slope</i> and <i>Slope/W</i>	44
Conclusions.....	49
Suggestions for Future Development.....	50
References.....	50

Appendix—A CD for computer program *Pf-slope*, executable file
Including input data files for Fruitgrowers and Ridgway Dams

Tables

<i>No.</i>		<i>page</i>
1	Deterministic soil properties used in the Fruitgrowers Dam pre- and postliquefaction analyses.....	27
2	Probabilistic soil properties used in the Fruitgrowers postliquefaction analyses.....	28
3	<i>CoV</i> values characterizing Fruitgrowers probabilistic runs.....	28

4	Isotropic θ values (ft) characterizing Fruitgrowers spatial variation of soil.....	29
5	Results from the Fruitgrowers probabilistic analyses run with Slope/W	32
6	Results from the Fruitgrowers probabilistic analyses run with <i>Pf-slope</i>	32
7	Deterministic soil properties used in Ridgway Dam pre- and postliquefaction analyses.....	42
8	Probabilistic soil properties used in Ridgway postliquefaction analyses	42
9	<i>CoV</i> values characterizing Ridgway probabilistic runs	43
10	Isotropic θ values (ft) characterizing Ridgway spatial variation of soil	43
11	Results from the Ridgway probabilistic analyses	47
12	Results from the Ridgway probabilistic analyses	47

Figures

<i>No.</i>		<i>page</i>
1	Data file section 1	9
2	Data file section 2	10
3	<i>Pf-slope</i> mesh representation of data entered in section 2 of the data file....	10
4	Direction of element counting for the creation of the data file.....	11
5	The coordinates' origin.....	12
6	Section 3 of the input data file describing the soil properties characterizing each random field.....	13
7	Section 4 of the input data file describing the program convergence accuracy	16
8	Section 5 of the input data file describing the water table conditions throughout the mesh.....	16
9	Section 6 of the input data file representing the user's output printing options.....	17
10	Section 1 of the data output file summarizing the analysis input data.....	18
11	Section 2 of the data output file summarizing the displacement computed by the program at each <i>SRF</i> trial.....	19
12	Section 3 of the data output file summarizing the deterministic value of <i>FS</i> , its statistical properties, and the <i>pf</i> computed by the program.....	19
13	(a and c) Node numbering of a right-sloping, degenerated, 8-node triangular element; (b) node numbering of a square, 8-node quadrilateral element.....	20
14	Representation of a typical mesh from <i>Pf-slope</i>	20
15	Typical nodal displacement vector representation from <i>Pf-slope</i>	20
16	Representation of a typical displaced mesh from <i>Pf-slope</i>	21
17	Representation of possible variation in spatial correlation in a random field	21
18	General plan view and cross sections of Fruitgrowers Dam.....	23
19	Geologic cross section along the maximum section of Fruitgrowers Dam ..	24

20 Deterministic postliquefaction analysis computed in 2004 using the software Slope/W version 7.4 25

21 Cross section G-G' showing postconstruction actual dimensions of Fruitgrowers Dam 26

22 Representation of the 2004 model used in the deterministic postliquefaction analysis..... 27

23 Variability in *pf* results using 1,000 Monte-Carlo simulations. To recognize how much the *pf* computed by the Fruitgrowers model could vary in a probabilistic setting, the same data file was run 50 times..... 29

24 .DIS file showing displacement associated with the deterministic preliquefaction conditions at Fruitgrowers Dam 30

25 Graphical representation according to Spencer's Method of the Slope/W results describing the deterministic preliquefaction conditions at Fruitgrowers Dam 30

26 .DIS file from *Pf-slope* showing displacement associated with the deterministic postliquefaction conditions at Fruitgrowers Dam 31

27 Graphical representation according to Spencer's Method of the Slope/W results describing the deterministic postliquefaction conditions at Fruitgrowers Dam 31

28 Comparison of the results from programs *Pf-slope* and Slope/W for both lower and higher *CoV*. *Pf-slope* results are based on the deterministic FS of 1.09 the and Slope/W results on the deterministic FS of 1.06..... 33

29 General plan view and cross sections of Ridgway Dam..... 38

30 Geologic cross section along the maximum section of Ridgway Dam 39

31 Representation of the 2008 model used in the deterministic postliquefaction analysis..... 41

32 .DIS file showing displacement associated with deterministic preliquefaction conditions at Ridgway Dam..... 44

33 Graphical representation according to Spencer's Method of the Slope/W results describing deterministic preliquefaction conditions at Ridgway Dam..... 44

34 Graphical representation according to Spencer's Method of the Slope/W results describing the deterministic postliquefaction conditions at Ridgway Dam when the liquefiable layer is assumed to be frictionless 45

35 .DIS file showing displacement associated with the deterministic postliquefaction conditions at Ridgway Dam when the liquefiable layer is assumed to be frictionless 45

36 .DIS file showing displacement associated with deterministic postliquefaction conditions at Ridgway Dam when a friction angle of 5° characterizes the liquefiable layer..... 46

37 Graphical representation according to Spencer's Method of the Slope/W results describing deterministic postliquefaction conditions at Ridgway Dam when a friction angle of 5° characterizes the liquefiable layer 46

38 Comparison of the results from *Pf-slope* and Slope/W for both lower and higher *CoV*. *Pf-slope* results are based on the deterministic FS of 0.98 the and Slope/W results on the deterministic FS of 1.07 48

Probabilistic Slope Stability Analysis Using the
Random Finite Element Method (RFEM)—Report of Findings

Introduction

Agencies working in the dam safety profession widely recognize the need to move toward probabilistic and risk-based methods for decision making.

For over a decade, the Bureau of Reclamation (Reclamation) has instituted risk-based guidelines for dam safety decision making moving toward this common trend.

Realistic risk assessment of embankment dams should be able to estimate the risk associated with all potential failure modes and loading states, and therefore, quantify the probability of failure related to each failure mode.

This report of findings presents a summary that outlines a robust methodology that has the ability to model risk in a wide range of slope instability cases where traditional methods are deficient due to their inability to properly characterize spatial variability. Furthermore, the elasto-plastic, finite element, slope stability approach at the root of this methodology makes no *a priori* assumptions about the shape or location of the critical failure mechanism and therefore, offers significant benefits over traditional limit equilibrium methods in the analysis of highly variable soils.

Scope

The scope of this research is to create a computer program (see appendix) based on the random finite element method (RFEM) (e.g., Fenton and Griffiths, 2008) able to estimate the probability of failure of slopes while fully accounting for spatial variability controlled through an input parameter called the *spatial correlation length*. In addition, this research has developed a methodology capable of estimating slope probability of failure without requiring the failure surface to be anticipated ahead of time, as is the case with other methods currently in use. The two key points mentioned above allow this methodology to deliver an improved estimate of slope probability of failure, which can represent a significant component toward a more precise risk assessment and therefore, a more informed and cost-effective dam safety modification alternative (e.g., Smith and Griffiths, 2004; Griffiths and Lane, 1999).

This report of findings outlines the key components of the computer program *Pf-slope*, created for this research project. A reasonable estimate of the likelihood of failure for slope stability mechanisms, especially in nonlinear analysis involving postearthquake liquefaction stability, is still one of the unknowns of the

risk evaluation conducted by Reclamation. Particular interest is given during this project to modeling of potential embankment structure instability caused by a seismic event. Nevertheless, the program could be used to model potential slope instability during construction or modification of a dam.

Program Description

Program Methodology and Theory

The starting point for the development of *Pf-slope* is in the probabilistic approach based on the random field theory developed by Griffiths and Fenton in 2004. This approach, called the random finite element method (RFEM), combines elasto-plastic finite elements analysis with random field theory generated using the local average subdivision method (e.g., Fenton and Vanmarcke, 1990; Fenton and Griffiths, 2008).

Slope stability theory

A brief description of the program methodology is given below. For more detailed information on the elasto-plastic (or visco-plastic) and strength reduction algorithms used in this study, the reader is referred to Griffiths and Lane (1999) and Smith and Griffiths (2004).

The main program, *Pf-slope*, coded in FORTRAN 95, requires a library created to execute the majority of the basic computations needed in the main program. The library is divided into three subsections called *geom*, *gaf95*, and *main*.

The section of the library called *geom*, which contains 11 subroutines, describes the geometry of the problem investigated and is instructed to compute nodal coordinates throughout the finite element mesh as well as node and element numbers.

The section of the library called *gaf95* contains 117 subroutines responsible for the probabilistic section of the program as well as the creation of a PostScript plot of the displaced mesh with an optional gray scale representing the material property random field.

The section of the library called *main* contains 144 subroutines and is responsible for the computations of elements, shape functions, local and global components of mass matrix, stiffness matrix, elastic and plastic stress-strain matrices, body load, gravity load, pore pressure, and all the numerical components needed to compute these parameters. In addition, *main* contains a subroutine called *dismsh* that generates a PostScript image of the deformed mesh without a gray scale, and a

subroutine called *vecmsh* that generates a PostScript image of the nodal displacement vectors.

The first section of *Pf-slope* is dedicated to the declaration of variables as integers, real numbers, and dynamic arrays that are later allocated to the program's body. The following section of the program, called "Input or initiation," assigns to each variable its value whether the value is specified in the program's main body or declared in a separate input data file. Subsequently, the program calculates the problem geometry from the dimensions entered in the data file, and all node and element numbers are assigned throughout the problem mesh. These operations are computed mainly outside of the program's main body in the program library section called *geom*. The program then loops through the elements' nodes and coordinates to find the global arrays sizes needed for the computation of pore pressures, gravity loads, body loads, and stiffness matrix.

The last part of this section of the main program calls two important subroutines at the base of the probabilistic analysis called *sim2sd1* and *sim2sd2*, which are stored in the section of the program library called *gaf95*. A subsequent part of the program is dedicated to the element stiffness integration and assembly calculations. In this section of the program, soil properties are read from the input data file and assigned to the embankment's and foundation's random fields. This section of the program can analyze a liquefiable layer in either the foundation, the embankment, or the partition of a homogeneous embankment into two materials. Clearly, these more complicated components depend highly on the problem analyzed and required modifications of the main program code each time a different problem is selected.

A series of subroutines (*deemat*, *shape_fun*, *bee8*, and *fsparv*) are successively called in the program to generate, in progression, the elastic stress-strain matrix, the shape functions at the integrating points, the analytical version of the stiffness matrix for an 8-node quadrilateral element, and the lower triangular global matrix, *kv*, stored as a vector in skyline form. Then the program calls a subroutine, *water_load*, that generates the additional loading due to freestanding water outside of the slope as well as a water surface within the slope. The water load is computed for each of the five sections forming the mesh and then added to the total load already computed and is equal to the sum of gravity load and pore pressure load. This subroutine allows for the analysis of submerged slopes as well as slopes characterized by a specific water table that can vary in elevation throughout the mesh.

The next sections of the main program compute the strength reduction factor and then perform a check on whether the yield is violated according to the failure criterion. The theory coded in this section of the program is described more in detail in the following paragraphs.

Pf-slope models a 2-dimensional strain analysis of elastically perfect plastic soils with a Mohr-Coulomb failure criterion using 8-node quadrilateral elements with

reduced integration (four Gaussian-points per element) in the gravity load generation, the stiffness matrix generation, and the stress redistribution phases of the algorithm. From the literature, conical failure criteria are the most appropriate to describe the behavior of soils with both frictional and cohesive components, and the Mohr-Coulomb criterion is known as the best of this group of failure criteria. Therefore, the program uses the Mohr-Coulomb criterion as the failure mechanism in all cases. In terms of principal stresses and assuming a compression-negative sign convention, the Mohr-Coulomb criterion can be written as follows:

$$F_{mc} = \frac{\sigma'_1 + \sigma'_3}{2} \sin \phi' - \frac{\sigma'_1 - \sigma'_3}{2} - c' \cos \phi' \quad (1)$$

where σ'_1 and σ'_3 are the major and minor principal effective stresses, respectively.

In cases where the soil is characterized by a frictionless component (undrained clays) the Mohr-Coulomb criterion can be simplified into the Tresca criterion substituting $\phi = 0$ in equation 1 and obtaining the following form,

$$F_t = \frac{\bar{\sigma}(\cos \theta)}{\sqrt{3}} - c_u \quad (2)$$

where $\bar{\sigma}$ = deviator stress in a triaxial test, and c_u = undrained cohesion.

The failure function, F , for both criteria can be interpreted as follows:

- $F < 0$: stresses inside failure envelope (elastic)
- $F = 0$: stresses on failure envelope (yielding)
- $F > 0$: stresses outside failure envelope (yielding and must be redistributed)

The soil is initially assumed to be elastic, and the model generates normal and shear stresses at all Gauss-points within the mesh. These stresses are then compared with the Mohr-Coulomb failure criterion.

The elastic parameters E' and ν' refer to the Young's modulus and Poisson's ratio of the soil, respectively, for the effective stress. If a value of Poisson's ratio is assumed (typical drained values lie in the range $0.2 < \nu' < 0.3$), the value of Young's modulus can be related to the compressibility of the soil as measured in a 1-dimensional odometer (e.g., Lambe and Whitman, 1969),

$$E' = \frac{(1 + \nu')(1 - 2\nu')}{m_v(1 - \nu')} \quad (3)$$

where m_v is the coefficient of volume compressibility.

In this study, the parameters E' and ν' have the values of $E' = 10^5$ kN/m² and $\nu' = 0.3$, respectively. The total unit weight, γ , assigned to the soil is proportional to the nodal self-weight loads generated by gravity. The forces generated by the self-weight of the soil are computed using a gravity procedure that applies to the slope of a single gravity increment.

The global gravity load vector (called *gravlo* in the program) for a material with unit weight γ is accumulated from each element by integration of the shape functions $[N]$ as follows,

$$\text{gravlo} = \sum_{\text{elems}}^{\text{all}} \gamma \iint [N]^T dx dy \quad (4)$$

which can also be written as follows,

$$\text{gravlo}^{(e)} = \gamma \int_{V^e} N^T dV^e \quad (5)$$

where N represents the shape functions of the element and the subscript e refers to the element number. This integral evaluates the volume of each element, multiplies by the total unit weight of the soil, and distributes the net vertical force consistently to all the nodes.

Others have shown that in nonlinear analyses, the stress paths due to sequential loading versus the path followed by a single increment to an initially stress-free slope can be quite different and produce different results; however, the factor of safety appears unaffected when using elasto-plastic models (e.g., Borja *et al*, 1990; Smith and Griffiths, 1998). It is also important to remember that classical limit equilibrium methods do not account for loading sequence in their solutions. The gravity load calculations are performed in the same part of the program that forms the global stiffness matrix. In the program library, the subroutine called *bee8* contains the algebraic version of the $[B]$ matrix (strain displacement matrix) for an 8-node quadrilateral element corresponding to any given local coordinate (ξ, η) . The $[B]$ matrix is then used in the stiffness computation. A general form of the stiffness matrix with a contribution from all four Gauss-points in the element is computed as follows,

$$[k_m] \approx \sum_{i=1}^4 W_i \det |J|_i \left([B]^T [D] [B] \right)_i \quad (6)$$

where $[B]$ and $[D]$ represent the strain-displacement and stress-strain matrices, respectively, W_i is a weighting coefficient, and $\det |J|$ is the determinant of the Jacobian matrix.

In the program, the application of gravity loading is followed by a systematic reduction in soil strength until failure occurs. This is achieved using a strength reduction factor SRF , which is applied to the frictional and cohesive components of strength in the form:

$$\phi'_f = \arctan\left(\frac{\tan \phi'}{SRF}\right) \quad \text{and} \quad c'_f = \frac{c'}{SRF} \quad (7)$$

The factored soil properties ϕ'_f and c'_f are the properties actually used in each trial analysis. When slope failure occurs, as indicated by an inability of the algorithm to find an equilibrium stress field that satisfies the Mohr-Coulomb failure criterion coupled with significantly increasing nodal displacements, the factor of safety is given by:

$$FS \approx SRF \quad (8)$$

In the literature, this method is referred to as the “shear strength reduction technique” (e.g., Smith and Griffiths, 1988; Matsui and San, 1992).

After the computation of reduction of soil strength, a subsequent section of the program computes the total body load vectors. A description of generation of body loads computed in the program is summarized in the following paragraph, but a more detailed description can be found in Smith and Griffiths (2004), especially regarding the algorithm used in the program involving visco-plasticity.

An elastic solution is repeated according to the constant stiffness method used in the program to achieve convergence by iteratively varying the loads on the system. Within each load increment, the system of equations,

$$[K_m]\{U\}^i = \{F\}^i \quad (9)$$

must be solved for the global displacement increments $\{U\}^i$, where i represents the iteration number, $[K_m]$ the global stiffness matrix, and $\{F\}^i$ the global external and internal body loads.

The element displacement increments $\{u\}^i$ are extracted from $\{U\}^i$, and these lead to strain increments via the element strain-displacement relationships:

$$\{\Delta\varepsilon\}^i = [B]\{u\}^i \quad (10)$$

Assuming the material is yielding, the strains will contain both elastic and (visco) plastic components; thus:

$$\{\Delta\mathcal{E}\}^i = \{\Delta\mathcal{E}^e\}^i + \{\Delta\mathcal{E}^p\}^i \quad (11)$$

and the stress component will be expressed using the following form:

$$\{\Delta\sigma\}^i = [D^e] \{\Delta\mathcal{E}^e\}^i \quad (12)$$

These stress increments are added to stresses already existing from the previous load step and the updated stresses substituted into the Mohr-Coulomb failure criterion (e.g., 1).

Stress redistribution, if necessary ($F > 0$), is done by altering the load increment vector $\{F\}^i$ in equation 9. Generally, the vector $\{F\}^i$ holds two types of load as shown in equation 13,

$$\{F\}^i = \{F_a\} + \{F_b\}^i \quad (13)$$

where $\{F_a\}$ is the applied external load increment, and $\{F_b\}^i$ is the body load vector that varies from one iteration to the next. Finally, the body load vector $\{F_b\}^i$ must be self-equilibrating so that it does not affect the net loading on the system.

After the computation of body load vectors is completed, the program calls two subroutines *vecmsh* and *dismsh3f*, from the section of the library called *main*, responsible for generating the graphical output files. These two subroutines generate, respectively, a PostScript image of the nodal displacement vectors and a PostScript image of the deformed mesh. The generation of the graphical output files completes the coding of the main program.

The following section is dedicated to the basic theory behind the probabilistic analysis computed by the program.

Probabilistic random theory

In *Pf-slope*, the probability of failure can be calculated using two different approaches. When the program is asked to compute the factor of safety (FS) for each Monte-Carlo simulation, the proportion of Monte-Carlo simulations with $FS < 1$ describes the probability of failure. When the program is asked to compute the probability without determining the exact value of FS for each simulation, the proportion of Monte-Carlo slope stability analyses that failed describes the probability of failure. In this case, the chosen state function is $FS = 1$, and the *SRF* is also equal to 1. "Failure" is said to have occurred if, for any given realization, the algorithm (Mohr-Coulomb failure criterion) was unable to converge within 500 iterations.

The RFEM code can generate a random field of shear strength values and map them onto the finite element mesh, taking full account of element size in the local

averaging process. In a random field, the value assigned to each cell (or finite element in this case) is itself a random variable.

The random variables can be correlated to one another by controlling the spatial correlation length and the cross-correlation matrix where the degree of correlation, ρ , between each property can be expressed in the range of $0 \leq \rho \leq 1$.

The correlation coefficient between two random variables X and Y can be defined by the form:

$$\rho_{XY} = \frac{CoV[X, Y]}{\sigma_x \sigma_y} \quad (14)$$

where the coefficient of variation, CoV , represents the covariance between the two variables X and Y and their respective standard deviations, σ_x and σ_y .

The spatial correlation length (θ), also referred to in literature as “scale of fluctuation,” describes the distance over which the spatially random values tend to be significantly correlated in the underlying Gaussian field. Mathematically, θ is defined as the area under the following correlation function (e.g., Fenton and Griffiths, 2008, from Vanmarcke, 1984):

$$\theta = \int_{-\infty}^{\infty} \rho(\tau) d\tau = 2 \int_0^{\infty} \rho(\tau) d\tau \quad (15)$$

where τ represents the distance between two positions in the random field. A large value of θ implies a smoothly varying field, while a small value implies a ragged field.

Another important dimensionless statistical parameter involved in this probabilistic approach is the coefficient of variation V , which, for any soil property, can be defined as:

$$V = \frac{\sigma}{\mu} \quad (16)$$

where σ is the standard deviation and μ the mean value of the property.

In brief, the analysis involves the application of gravity loading and the monitoring of stresses at all the Gauss-points. The slope stability analysis uses an elastically perfect plastic stress-strain law with a Mohr-Coulomb failure criterion. If the Mohr-Coulomb criterion is violated, the program attempts to redistribute excess stresses to neighboring elements that still have reserves of strength. This is an iterative process that continues until the Mohr-Coulomb criterion and global equilibrium are satisfied at all points within the mesh under quite strict tolerances.

Plastic stress redistribution is accomplished using a visco-plastic algorithm with 8-node quadrilateral elements and reduced integration in both the stiffness and stress redistribution parts of the algorithm. For a given set of input shear strength parameters (mean, standard deviation, and spatial correlation length), Monte-Carlo simulations are performed until the statistics of the output quantities of interest become stable.

A more comprehensive explanation of the random finite elements method, including local averaging approach and discussion on spatial correlation length, can be found in Griffiths and Fenton (2008).

Input File Description

Pf-slope can be used to compute a deterministic slope stability analysis or a probabilistic slope stability analysis. A general data file created to hold the data required by the main program can be subdivided into seven main sections.

The first section (figure 1) contains the name of the analysis, and the mode on which the analysis will be performed. The user can choose between two analyses. One analysis returns the exact FS values with their statistical properties (minimum, maximum, mean, and standard deviation) and the probability of $FS < 1$, or nonconvergence (*pf*). A second, less computational and therefore, faster analysis returns the *pf*, where the FS and the *SRF* are set to be equal to 1, and a simple fail/no-fail evaluation characterizes the FS without going through the calculation of the exact FS value. The first user option is associated with the number 1 while the second, less computational option is associated with the number 0.

The second section of the input data file (figure 2) can be considered the “geometry input section,” in which all the data describing the geometry of the problem of interest are stored. Figure 3 shows a graphical representation of the data entered in this section of the data file.

```
'2d random slope'

Factor of Safety analysis or a simple failure analysis
  (ifsa=1 FS, ifsa=0 Failure)
1
```

Figure 1.—Data file section 1.

Probabilistic Slope Stability Analysis Using the
Random Finite Element Method (RFEM)—Report of Findings

```

dx, lfgrad, rtgrad, nex1, nex2, nex3, ney1, ney2, ney3
1 3.5 2.5 16 5 16 6 6 3
nex4, nex5, ney5, ney6 (weak layer)
0 67 2 3

nbf
3
    
```

Figure 2.—Data file section 2.

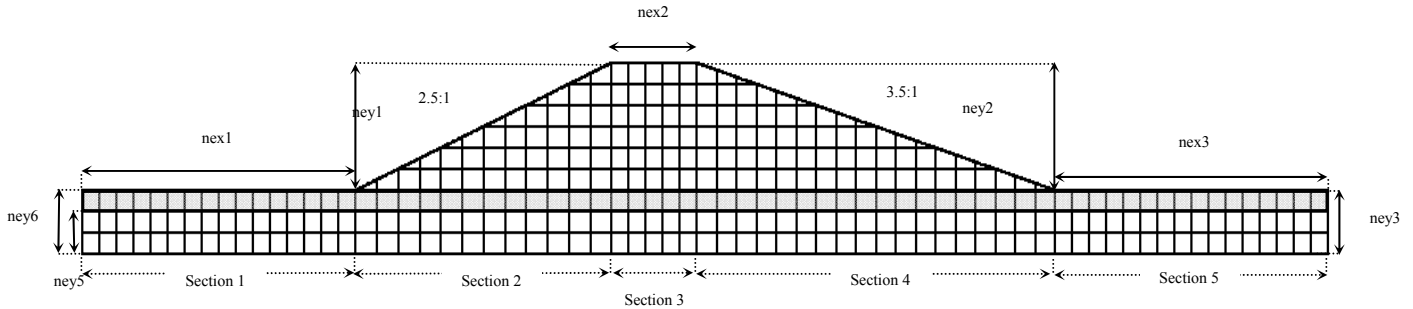


Figure 3.—*Pf*-slope mesh representation of data entered in section 2 of the data file.

The first line of this section requires the user to enter, in order, the following data:

- dx , the size of the square element
- $rtgrad$, the gradient of the downstream slope
- $lfgrad$, the gradient of the upstream slope
- $nex2$, the number of elements forming the embankment in the x direction
- $nex3$, the number of elements characterizing the downstream section in the x direction
- $nex1$, the number of elements characterizing the upstream section in the x direction
- $ney2$, the number of elements characterizing the height of the embankment in the downstream section
- $ney3$, the number of elements characterizing the thickness of the foundation in the downstream section
- $ney1$, the number of elements characterizing the height of the embankment in the upstream section
- nbf , the number of rows characterized by the foundation properties

The second line of this section, relative to the geometry data of a weak layer located either in the foundation or in the embankment, requires the user to enter, in order, the following data:

- *nex4*, the number of elements before the starting of the weak zone in the x direction
- *nex5*, the number of elements at the end of the weak zone in the x direction
- *ney5*, the number of elements before the starting of the weak zone in the y direction
- *ney6*, the number of elements at the end of the weak zone in the y direction

The direction of element numbering progresses in the program from the mesh top to bottom and left to right, while the direction of element counting for the creation of the data file is shown in figure 4. The coordinates' origin is shown in figure 5.

The last line of this section asks the user to enter the number of elements in the y direction, to which the program assigns foundation material properties (*nbf*).

The third section of the input data file (figure 6) groups all the material properties and the correlations among properties (*correlation matrix*) used in each of the two random fields generated in the program. The first random field describes the embankment properties while the second random field describes the foundation properties. The properties characterizing the weak layer/zone actually assume the statistical properties of the random field in which the weak layer/zone is located (embankment or foundation), with the exception of the mean values that the user will have to code into the main program.

The soil model coded in the program consists of six parameters, cohesion (*c*), friction angle (*phi*), dilation angle (*psi*), unit weight (*gam*), Young's modulus (*e*), and Poisson's ratio (*v*). This program, based on an elasto-plastic model, uses a constant dilation angle of $\psi = 0$, assuming zero volumetric change during yield. The reason for the assumption of a dilation angle of $\psi = 0$ is that if $\psi = \phi'$, then the

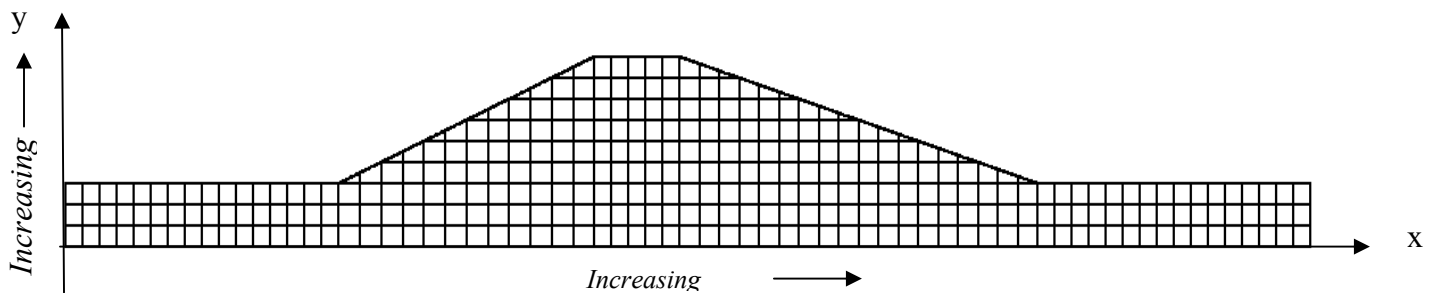


Figure 4.—Direction of element counting for the creation of the data file.

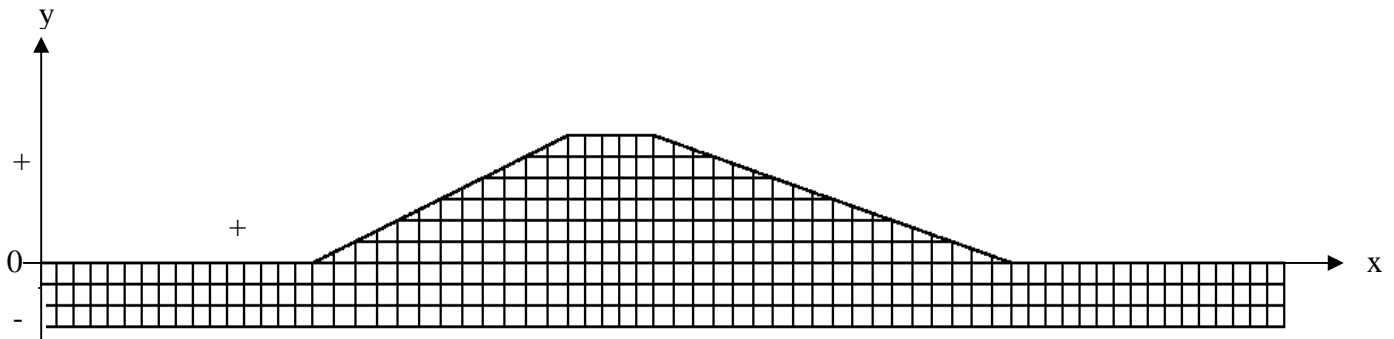


Figure 5.—The coordinates' origin.

plasticity flow rule is “associated,” and it is well known that the use of an “associated” flow rule in frictional soil models predicts far greater dilation than those observed in reality, leading to increased failure load prediction. For this reason, a “nonassociated” flow rule is preferred for this model following the steps of other successful constitutive soil models (e.g., Molenkamp, 1981; Griffiths, 1982; Hicks and Boughrarou, 1998). In this research, Young’s modulus (E) and Poisson’s ratio (ν) possess the deterministic values of 10^5 kN/m², and 0.3, respectively.

As shown in figure 6, a real array with dimensions of at least 7 by 6 contains the six parameters characterizing the soil model. Each of the six parameters characterizing the soil model can be treated either as deterministic or probabilistic. If any of the six properties after the first value representing the property mean are considered in a probabilistic fashion, the user will enter the properties’ standard deviations and distribution types. Options 3 and 4 in the distribution type require additional input instead of, or in addition to the traditional mean and standard deviation as explained below.

The user chooses a number between 0 and 4 to characterize the desired distribution according to the following options:

- 0.0 If the property is deterministic (at mean value)
- 1.0 If the property is normally distributed
- 2.0 If the property is lognormally distributed
- 3.0 If the property is described by a bounded distribution, the first and second values describing the property are ignored, and the four parameters after the distribution type input completely describe the distribution as follows:

4th parameter = lower bound (bounded), or mean of log-process (logn)

```

c phi psi gam e v properties of embankment (mean, SD,
dist, L, U, m, s)
432.0    0.0    0.0    0.0    0.0    0.0    0.0
 32.0    0.0    0.0    0.0    0.0    0.0    0.0
  0.0    0.0    0.0    0.0    0.0    0.0    0.0
126.0    0.0    0.0    0.0    0.0    0.0    0.0
1.e5     0.0    0.0    0.0    0.0    0.0    0.0
0.3      0.0    0.0    0.0    0.0    0.0    0.0

Correlation matrix
1.0  0.0  0.0  0.0  0.0  0.0
0.0  1.0  0.0  0.0  0.0  0.0
0.0  0.0  1.0  0.0  0.0  0.0
0.0  0.0  0.0  1.0  0.0  0.0
0.0  0.0  0.0  0.0  1.0  0.0
0.0  0.0  0.0  0.0  0.0  1.0

continue

c phi psi gam e v properties of foundation (mean, SD,
dist, L, U, m, s)
32.0     0.0    0.0    0.0    0.0    0.0    0.0
23.0     0.0    0.0    0.0    0.0    0.0    0.0
 0.0     0.0    0.0    0.0    0.0    0.0    0.0
128.0    0.0    0.0    0.0    0.0    0.0    0.0
1.e5     0.0    0.0    0.0    0.0    0.0    0.0
0.3      0.0    0.0    0.0    0.0    0.0    0.0

Correlation matrix
1.0  0.0  0.0  0.0  0.0  0.0
0.0  1.0  0.0  0.0  0.0  0.0
0.0  0.0  1.0  0.0  0.0  0.0
0.0  0.0  0.0  1.0  0.0  0.0
0.0  0.0  0.0  0.0  1.0  0.0
0.0  0.0  0.0  0.0  0.0  1.0

Spatial correlation length of embankment
480.0 480.0

Spatial correlation length of foundation
480.0 480.0

Random seed, number of simulations
  0  1

Covariance function name
dlavx2

```

Figure 6.—Section 3 of the input data file describing the soil properties characterizing each random field.

5th parameter = upper bound (bounded), or standard deviation of log-process (logn)

6th parameter = m parameter (if bounded)

7th parameter = s parameter (if bounded)

- 4.0 If the mean and standard deviation of the property change linearly (in which case the property is assumed to be lognormally distributed); also if the 1st, 2nd, and 4th data inputs of the property are, respectively, (1) the gradient of the trend that describes the property, (2) the value at the top of the trend that describes the property, and (4) the CoV , which is assumed to be constant. All the other values in that line are set to zero.

The probabilistic input description listed above applies equally to both random fields.

The second group of inputs in this section describes the correlation among the six soil properties using a 6-by-6 real array (*correlation matrix*). In the correlation matrix, the degree of correlation, ρ , between each property can be expressed in the range of $0 \leq \rho \leq 1$.

Throughout this study, the properties are actually assumed to be noncorrelated in both random fields.

The following group of inputs in this section represents the spatial correlation length value that the user needs to identify for both the embankment and foundation random fields. For each random field, the first and second real numbers characterize, respectively, the spatial correlation length in the x and the y directions. Two observations are important in the determination of these values. The first one is that the dimensions of the random fields are larger than those of the mesh, and the second one is that local averaging can significantly influence the pf result if the value of spatial correlation length is equal to or smaller than the size of the elements themselves. More detailed information about spatial correlation length is available in Griffiths and Fenton (2004). Guidelines on how to select values of spatial variation length from laboratory tests are available in the work conducted by Phoon and Kulhawy, *Characterization of geotechnical variability* (1999).

After the spatial correlation length inputs, the user needs to specify, in the following order, the two parameters of random seed number and number of Monte-Carlo simulations desired in the analysis. A specific random seed number can be used if the user wants to retest the results of a case of interest. Most commonly, the random seed in a probabilistic analysis can be set to 0.

The last input of this section refers to the selection of a covariance function. The user can select among five different covariance functions:

1. *dlavx2*: This is a Markovian covariance function. That is, the covariance between points in the field decays exponentially with absolute distance between the points:

$$r(X,Y) = var[\exp(-\tau)] \quad (17)$$

where *var* is the point variance, and τ is the absolute scale distance between the points:

$$\tau = \sqrt{2\left(\frac{X}{d\theta_x}\right)^2 + 2\left(\frac{Y}{d\theta_y}\right)^2} \quad (18)$$

where $d\theta_x$ and $d\theta_y$ are the scales of fluctuation in the x and y directions, respectively. If $var < 0$, then this function returns the variance of a local average of the process, $|var|V(X,Y)$, averaged over the domain XY . This variance is obtained by 16-point Gauss quadrature integration of the covariance function.

2. *dlsep2*: This is a separable Markovian covariance function. That is, the covariance between points in the field decays according to the product of the 2-directional, 1-dimensional Markovian covariance functions $r(X,Y) = var[r(X)*r(Y)]$.
3. *dlsp2*: This is a separable covariance function that decays exponentially with the squared distance between two points (a Gaussian type covariance function). The covariance function has the form $r(X,Y) = var[r(X)*r(Y)]$.
4. *dlaf2*: This is an approximately isotropic fractional Gaussian noise, or self-similar process.
5. *dl sfr2*: This is a separable fractional Gaussian noise covariance function, $r(X,Y) = var[r(X)*r(Y)]$.

In all five cases explained above, the parameter *var* represents the point variance of the property.

The most commonly used correlation function is *dlavx2*, primarily because of its simplicity, and it is the default function throughout this research.

The fourth section of the input data file (figure 7) asks the user to identify the parameters characterizing the convergence accuracy in the analysis. Throughout this study, the two parameters *Iteration ceiling* and the *Factor of safety accuracy tolerance* possess, respectively, values of 500 and 0.05.

```
Iteration ceiling
500

Factor of Safety accuracy tolerance
0.05
```

Figure 7.—Section 4 of the input data file describing the program convergence accuracy.

The fifth section of the input data file (figure 8) requires the user to enter information on the water table elevation throughout the mesh and the value of the unit weight of water.

These values can be expressed in either the Imperial or Metric system, as long as the unit system is compatible with the one used for the material properties and dimension input.

In the description of the water table, the first integer value represents the total number of free surface points that describe the water table. The following sets of real numbers represent the x and y coordinates of each point, respectively. If a dry condition characterizes the problem of interest, the user just needs to input the number of free surface points equal to 0, and the program requires no further specifications of coordinates. In the example shown in figure 8, the coordinates of the water table points as well as the unit weight are expressed using the inch-pound system. The program allows analysis of a dry condition, as well as a submerged case or a case with a general water table through the modeled structure.

The sixth and last section of the input data file (figure 9) requires the user to select which outputs need to be represented graphically. The first integer value of this section represents the number of random variables to be printed, which could be 1 to 6.

```
Number of free surface points and their coordinates
(nosurf, surf(:,nosurf))
5
  0.0    28.0
195.0    28.0
314.0    -7.0
480.0    -7.0
471.0    -7.0

Unit weight of water (gam_w)
62.4
```

Figure 8.—Section 5 of the input data file describing the water table conditions throughout the mesh.

```

Number of random variables to be printed (nrvp)
1
nrvp random variable No.
1
Plot log values (1) or actual values (0) of random
variable (rvd)
1

```

Figure 9.—Section 6 of the input data file representing the user’s output printing options.

The second integer value represents the type of property to be printed following this order:

1. Cohesion
2. Friction
3. Dilation angle
4. Unit weight of water
5. Young’s modulus
6. Poisson’s ratio

The last integer value allows the user to graphically show the actual property values by selecting 0, or the logarithmic values of the random property by selecting 1.

Data Output File Description

A general data output file (.RES), created to hold the analysis results run by the program, can be subdivided into three main sections.

The first section (figure 10) contains a summary of all the data input already discussed in the previous sections.

The second section (figure 11) of the data output file reports the total number of equations computed, the value of skyline storage, the starting random seed selected by the program, and the displacement data calculated in the analysis. The user can see the amount of displacement relative to each *SRF* trial and the number of iterations necessary to obtain convergence in the solution.

The third and last section of the data output file (figure 12) reports the deterministic estimate of the factor of safety as well as the factor of safety statistics and the computed probability of $FS < 1$, or nonconvergence (*pf*). The data output file also reports the number of simulations run by the analysis and the seed relative to the maximum and minimum values of safety factor. The example

Probabilistic Slope Stability Analysis Using the
Random Finite Element Method (RFEM)—Report of Findings

```
'2d random slope'
Factor of Safety analysis
dx,ltgrad,rtgrad,nex1,nex2,nex3,ney1,ney2,ney3
3. 3. 2. 37 6 54 12 12 12
nex4, nex5, ney5, ney6 (week layer)
0 92 10 12
Nbf
12
160 12
160 12
c phi psi gam e v properties of embankment (mean, SD, dist, L, U, m, s)
432. 0. 0. 0. 0. 0. 0. 0.
32. 0. 0. 0. 0. 0. 0. 0.
0. 0. 0. 0. 0. 0. 0. 0.
128. 0. 0. 0. 0. 0. 0. 0.
100000. 0. 0. 0. 0. 0. 0. 0.
0.3 0. 0. 0. 0. 0. 0. 0.
Correlation matrix
1.00 0.00 0.00 0.00 0.00 0.00
0.00 1.00 0.00 0.00 0.00 0.00
0.00 0.00 1.00 0.00 0.00 0.00
0.00 0.00 0.00 1.00 0.00 0.00
0.00 0.00 0.00 0.00 1.00 0.00
0.00 0.00 0.00 0.00 0.00 1.00
c phi psi gam e v properties of foundation (mean, SD, dist, L, U, m, s)
1. 0. 0. 0. 0. 0. 0. 0.
30. 0. 0. 0. 0. 0. 0. 0.
0. 0. 0. 0. 0. 0. 0. 0.
130. 0. 0. 0. 0. 0. 0. 0.
100000. 0. 0. 0. 0. 0. 0. 0.
0.3 0. 0. 0. 0. 0. 0. 0.
Correlation matrix
1.00 0.00 0.00 0.00 0.00 0.00
0.00 1.00 0.00 0.00 0.00 0.00
0.00 0.00 1.00 0.00 0.00 0.00
0.00 0.00 0.00 1.00 0.00 0.00
0.00 0.00 0.00 0.00 1.00 0.00
0.00 0.00 0.00 0.00 0.00 1.00
Spatial correlation length of embankment
480. 480.
Spatial correlation length of foundation
480. 480.
Random seed, number of simulations
0 1
Covariance function name
dlavx2
Iteration ceiling
500
Factor of Safety tolerance
0.050
Free-surface coordinates
0.00 28.00
195.00 28.00
314.00 -7.00
480.00 -7.00
471.00 -7.00
continue

Number of random variables to be printed
1
nrvp random variable No.
1
Plot log values (1) or actual values (0) of random variable
1
```

Figure 10.—Section 1 of the data output file summarizing the analysis input data.

```

There are 14124 equations and the skyline storage is 1204908
Starting seed 3946
trial factor      max displ      iterations
  0.5000      0.26841E+01          23
  1.0000      0.34365E+01         148
  1.0625      0.36395E+01         230
  1.0781      0.37374E+01         356
  1.0938      0.40547E+01         500
    
```

Figure 11.—Section 2 of the data output file summarizing the displacement computed by the program at each *SRF* trial.

```

Estimated Factor of Safety
                    1.09
Simulation   Random number   FS_max
           1           3946           1.09
Simulation   Random number   FS_min
           1           3946           1.09
           Pf      mean (FS)   SD (FS)
           0.0000           1.09           Na
    
```

Figure 12.—Section 3 of the data output file summarizing the deterministic value of *FS*, its statistical properties, and the *pf* computed by the program.

shown in figure 12 represents a deterministic analysis characterized by one, single simulation. For this reason, the same value represents the minimum, maximum, and mean of the *FS*, the Standard deviation value cannot be computed, and the *pf* for the single value of $1.09 > 1$ is equal to 0.0 percent.

Graphical Outputs

In addition to the output file summarizing the analysis results, *Pf-slope* generates three graphical representations of the slope, respectively contained in a .MSH .VEC, and .DIS file. The first file, .MSH, shows the problem mesh drawn by the program according to geometric inputs stored in the data file.

Eight-node quadrilateral elements characterize a typical finite element mesh produced by *Pf-slope*. The majority of the elements are square; however, the elements adjacent to the slope are degenerated into triangles and a general quadrilateral as shown in figure 13.

Five major sections—three horizontal and two sloping—characterize a general geometry model for an embankment dam (figure 14). Figure 14 shows a typical mesh that the new program *Pf-slope* can generate.

The second file, .VEC, displays the nodal displacement vectors corresponding to the unconverged solution (figure 15). The representation of the vectors,

Probabilistic Slope Stability Analysis Using the
Random Finite Element Method (RFEM)—Report of Findings

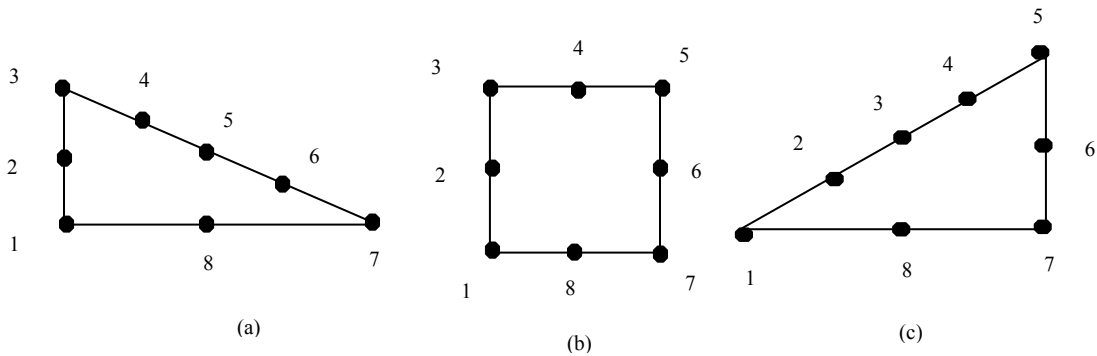
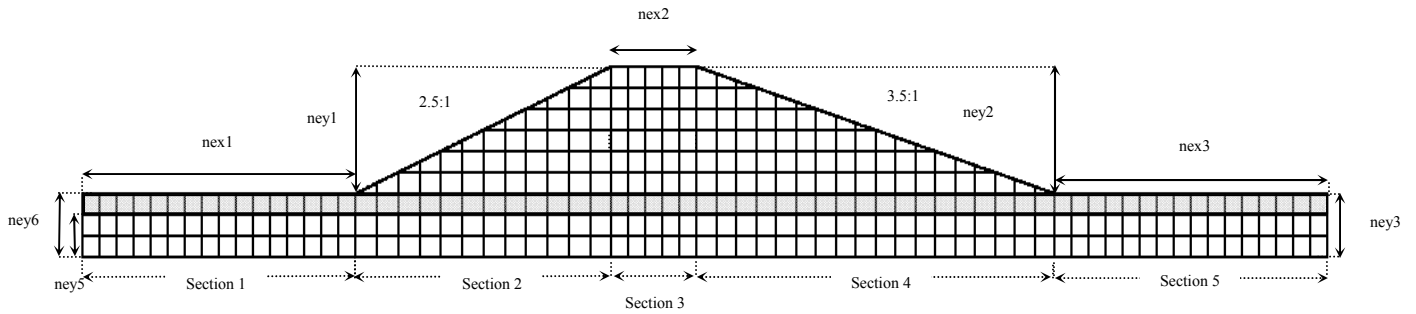


Figure 13.—(a and c) Node numbering of a right-sloping, degenerated, 8-node triangular element; (b) node numbering of a square, 8-node quadrilateral element.



Symbol legend:

- $nex1$ = number of elements in the x direction in the upstream horizontal section
- $ney1$ = number of elements in the y direction in the upstream embankment sloping section
- $nex2$ = number of elements in the x direction in the horizontal embankment section
- $ney2$ = number of elements in the y direction in the downstream embankment sloping section
- $nex3$ = number of elements in the x direction in the downstream horizontal section
- $ney3$ = number of elements in the y direction in the downstream foundation
- $ney5$ = number of elements below the bottom of the weak layer
- $ney6$ = number of elements below the top of the weak layer

Figure 14.—Representation of a typical mesh from *Pf-slope*.

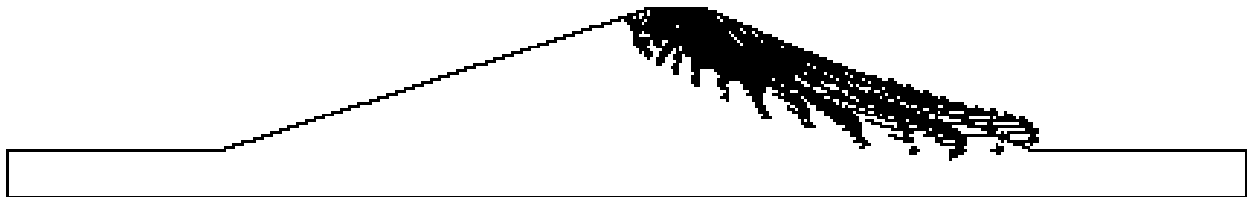


Figure 15.—Typical nodal displacement vector representation from *Pf-slope*.

controlled by a subroutine present in the main program, can be changed by varying a scaling factor based on the maximum nodal displacement.

The third file .DIS displays the deformed finite element mesh. Figure 16 shows a typical deformed mesh that the new program *Pf-slope* can generate.

A gray-scale representation of the material property random field is overlain onto the mesh to allow a better representation of the soil variability. It is important to remember that a large value of θ implies a smoothly varying field, while a small value implies a ragged field. Figure 17 shows an example of possible variation of spatial correlation in a random field.

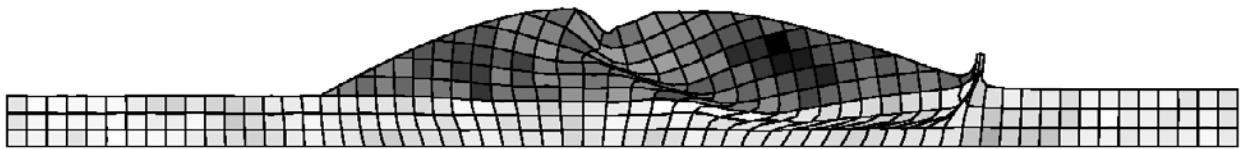


Figure 16.—Representation of a typical displaced mesh from *Pf-slope*.

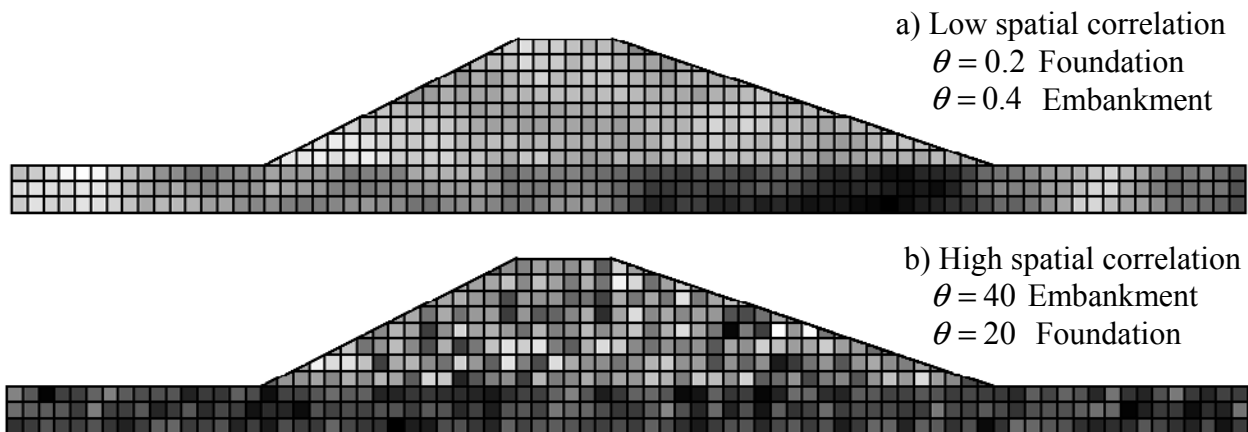


Figure 17.—Representation of possible variation in spatial correlation in a random field.

Case History Probabilistic Analysis

Fruitgrowers Dam

Fruitgrowers Dam is located in Delta County, 4 miles upstream from Austin, Colorado on Alfalfa Run, a tributary of the Gunnison River. Reclamation constructed the dam from 1938 to 1939 with the primary purpose of irrigation. The crest of the dam is at elevation 5493.0 feet. The dam has a structural height of 55 feet, hydraulic height of 40 ft, crest width of 25 feet, and crest length of 1,520 feet. The general plan view and cross sections of the dam are shown in figure 18.

The dam is a compacted, zoned earthfill structure consisting of a wide central zone 1 protected by a riprap layer on the upstream slope and by a thin gravel shell on the downstream slope. The embankment core is composed of clay, sand, and gravel, grading to gravel at the outer slopes. The embankment material was placed in 6-inch thick horizontal layers after rolling. Each layer was compacted with 12 passes of a compacting roller. Mechanical tampers were used near the abutments and concrete structures. A cut-off trench was excavated to impermeable material. The trench has a bottom width of 8 feet and is located 35 feet upstream of dam centerline.

The surficial material beneath the dam shell upstream and downstream of the cut-off trench was stripped to remove topsoil and organic material.

Figure 19 shows a geologic cross section along the maximum section of the dam.

More information on the geology and engineering properties of the embankment and the foundations at the site are available in the Technical Memoranda Nos. FW-8312-2 and FW-8312-3 by Reclamation (2004).

Background analyses

The case history of Fruitgrowers Dam was selected for this research because studies of the site conducted by Reclamation presented possible postearthquake liquefiable conditions in the foundation. To evaluate the liquefaction potential of the foundation, an investigation was conducted in 1980, and as a result of this investigation, the foundation liquefaction was not considered a problem because of the high blow counts and high clay content characterizing the site.

In 1998, a reevaluation of the data produced by the 1980 exploration showed the existence of silty sand (SM) soils in the right abutment area, and this discovery raised more questions on the performance of the site under liquefaction potential. To address this concern, a study was conducted in August 2004 using new data collected from five field explorations conducted between 1980 and 1999.

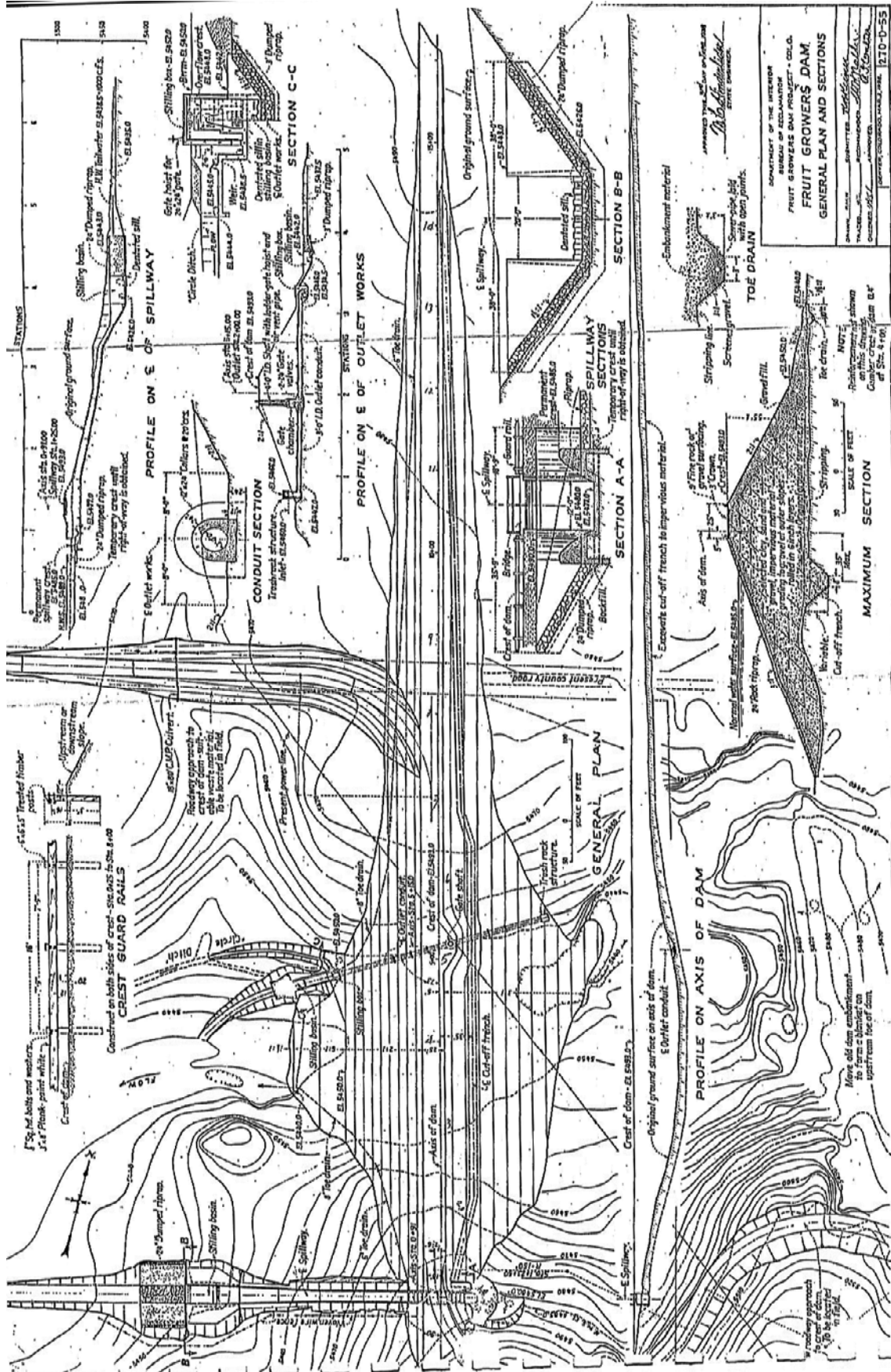


Figure 18.—General plan view and cross sections of Fruitgrowers Dam.

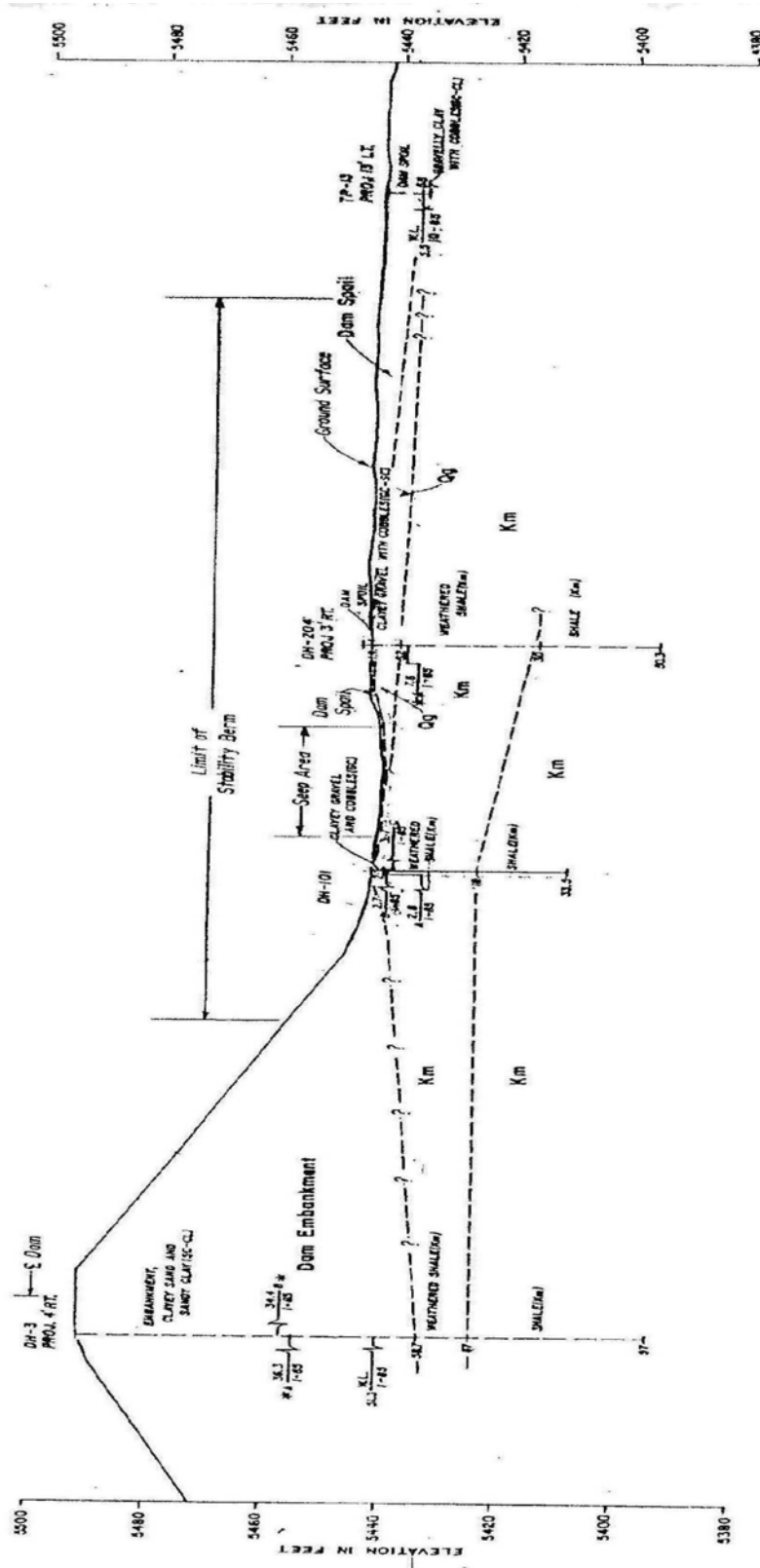


Figure 19.—Geologic cross section along the maximum section of Fruitgrowers Dam.

The results of this latest study showed a low likelihood of foundation liquefaction at the damsite. According to this study, to produce the failure of the embankment, a liquefied continuous lens larger than 64 feet should be present in the foundation under the right abutment. From the drill log data collected on each side of the embankment during the field explorations, the presence of such a long, continuous layer is unlikely. As shown in figure 20, a deterministic postliquefaction FS of 1.05 was computed for the structure assuming the presence of a 60-foot long liquefiable layer. From the computer program SLOPE/W version 7.4 the method of analysis used to compute this result was Spencer's Method, coupled with a rigid block theory technique for the evaluation of the failure surface.

Current analyses

In the *Evaluation of Liquefaction and Postearthquake Stability* conducted by Reclamation in August 2004, as well as in previous studies, the dam is essentially modeled as a homogeneous embankment. Similarly to the study conducted in 2004 the geometry of the current model is based on cross section G-G' shown in figure 21 (postconstruction actual dimensions) and also represents a homogeneous embankment. The phreatic condition characterizing the analysis is also adopted from the model constructed in 2004, which shows the reservoir elevation at 5485 feet (top of active conservation) with 8 feet of freeboard, and a downstream toe water elevation of 5453 feet, 4 feet below ground surface. This piezometric line was developed during a study also conducted in 2004 investigating the effect of the artesian pressure on the site foundation and embankment structure (Technical Memorandum No. FW-8312-2, 2004)

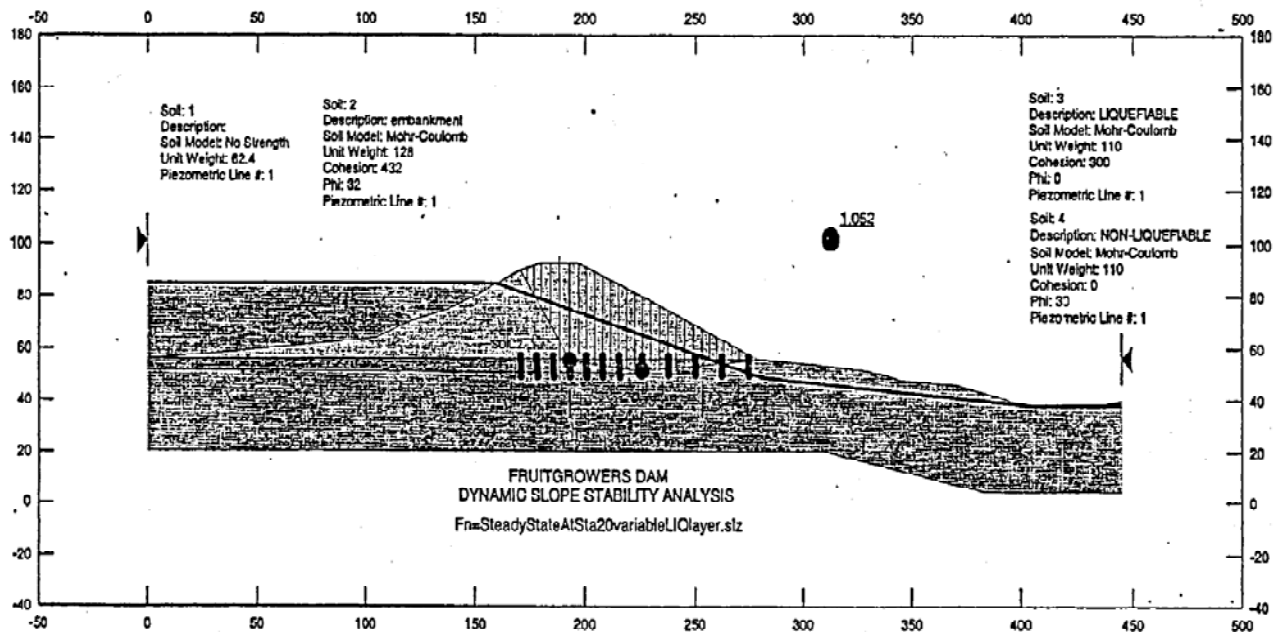


Figure 20.—Deterministic postliquefaction analysis computed in 2004 using the software Slope/W version 7.4.

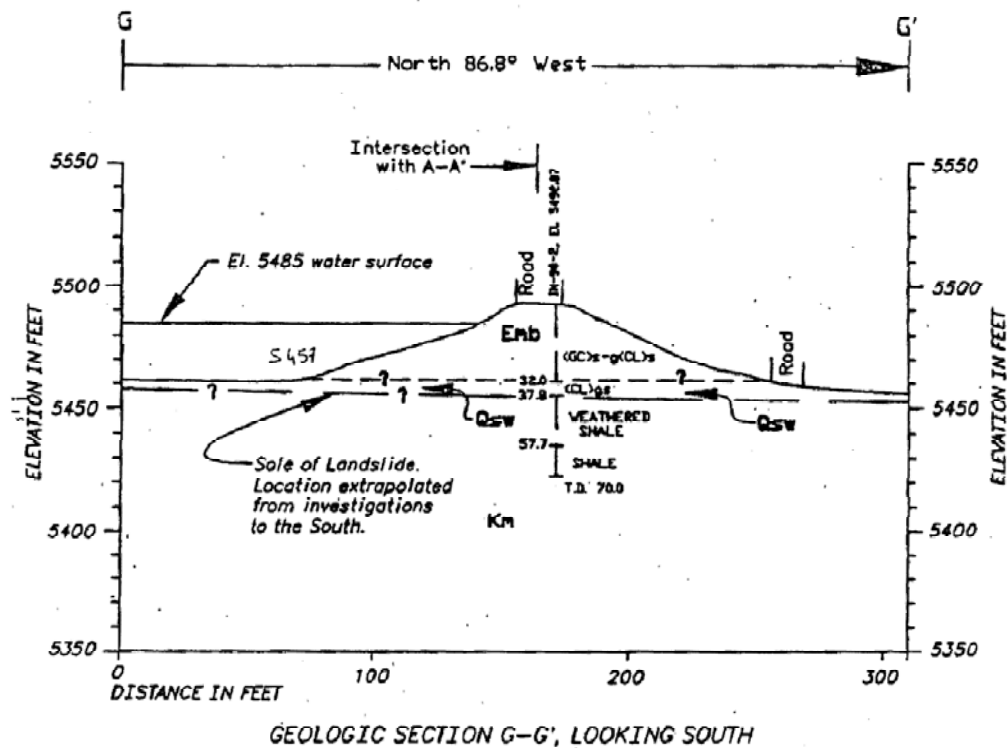


Figure 21.—Cross section G-G' showing postconstruction actual dimensions of Fruitgrowers Dam.

Figure 22 shows the piezometric line, the geometry, and the major units characterizing the deterministic model created in 2004.

The following three soil materials characterize the model representing Fruitgrowers Dam. The embankment core is composed of clay, sand, and gravel, grading to gravel at the outer slope. The foundation material consists of the Mancos Shale Formation (Km) and is modeled with a thickness of 36 feet. The Quaternary alluvium (Qal) is characterized by recent alluvial deposits of Alfalfa Run and is modeled with a thickness of about 6 feet.

Before diving into the probabilistic analysis, initial deterministic static analyses that modeled pre- and postliquefaction conditions were conducted using *Pf-slope*.

The soil properties used in the 2004 slope stability analysis to characterize the embankment, foundation, and liquefiable layer in the foundation are considered generally appropriate for these two deterministic analyses and are summarized in table 1.

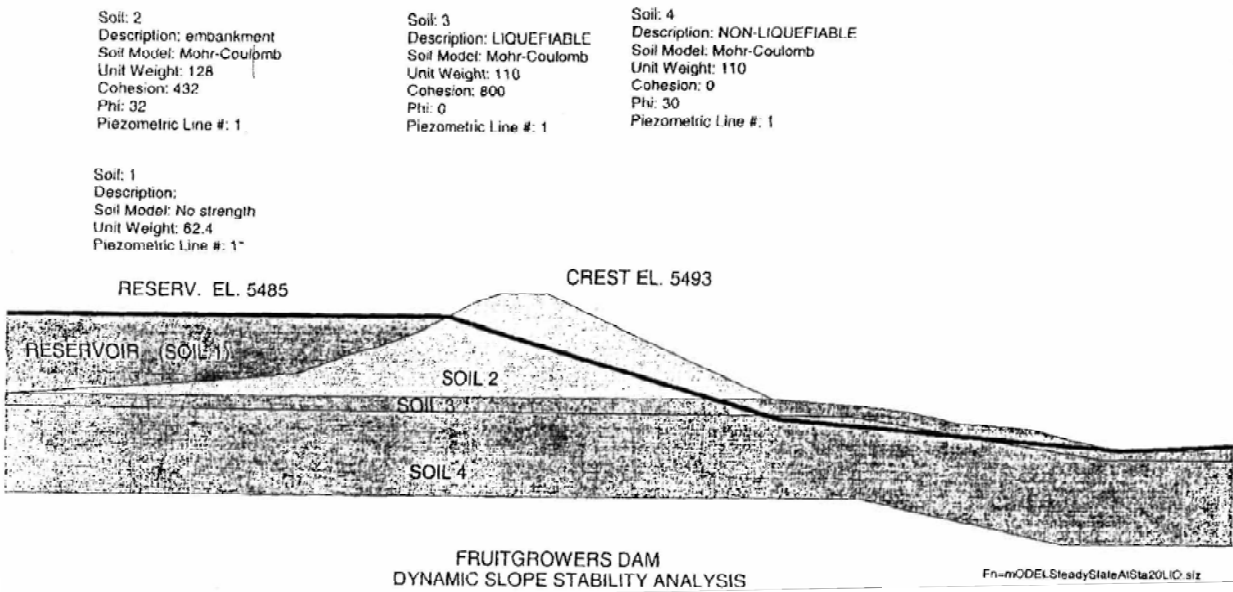


Figure 22.—Representation of the 2004 model used in the deterministic postliquefaction analysis.

Table 1.—Deterministic soil properties used in the Fruitgrowers Dam pre- and postliquefaction analyses

Liquefaction condition	Material	Unit weight (lb/ft ³)	ϕ' (°)	Cohesion c' (lb/ft ²)
Postliquefaction	Embankment	128	32	432
	Foundation	130	30	1
	Quaternary alluvium	130	0	300
Preliquefaction	Embankment	128	32	432
	Foundation	130	30	1
	Quaternary alluvium	130	30	1

The results from these deterministic analyses as well as the comparison with the results generated by Slope/W version 7.14 currently used by Reclamation are described in the next section, *Fruitgrowers deterministic and Probabilistic results comparison between Pf-slope and Slope/W programs.*

Subsequently the postliquefaction deterministic model was run using the probabilistic capability offered by *Pf-slope*. The soil properties as probabilistic variables and their statistical parameters used during the probabilistic analysis are summarized in table 2.

Table 2.—Probabilistic soil properties used in the Fruitgrowers postliquefaction analyses

Material	Mean	Standard deviation, lower CoV	Standard deviation, higher CoV	Distribution type
Embankment phi (°)	32	3.2	6.4	lognormal
Embankment cohesion (lb/ft ²)	432	43.2	86.4	lognormal
Foundation phi (°)	30	6	15	lognormal
Foundation cohesion (lb/ft ²)	1	0.2	0.5	lognormal
Quaternary alluvium phi (°)	0	0.2	0.5	lognormal
Quaternary alluvium cohesion (lb/ft ²)	300	60	150	lognormal

The probabilistic analysis associates one random field with the embankment and one with the foundation, and the liquefiable layer is described by the foundation random field, which is modified to address the new values describing the liquefiable material. In this probabilistic model, only the strength parameters of friction and cohesion are analyzed in a probabilistic approach; the other parameters—dilation angle, unit weight, Young’s modulus, and Poisson’s ratio—are analyzed with a deterministic approach.

To address the level of uncertainty incorporated in the mean values describing the properties, the same probabilistic model is run one time with a higher *CoV* and one time with a lower *CoV*. The *CoV* values used in each analysis for all material types are summarized in table 3

Table 3.—*CoV* values characterizing Fruitgrowers probabilistic runs

Material	Lower CoV	Higher CoV
Embankment phi (°) and cohesion (lb/ft ²)	0.1	0.2
Foundation phi (°) and cohesion (lb/ft ²)	0.2	0.5
Quaternary alluvium phi (°) and cohesion (lb/ft ²)	0.2	0.5

The *CoV* values characterizing the probabilistic analyses were chosen by evaluating suggested values available in the literature for similar soil material (e.g., Phoon and Kulhawy, 1999).

Another critical value in the analysis is the spatial correlation length used to determine the soil spatial variability. The set of isotropic values chosen to investigate the spatial correlation length θ for all probabilistic runs is reported in table 4.

Table 4.—Isotropic θ values (ft) characterizing Fruitgrowers spatial variation of soil

4
25
60
100
200
300
500

All the probabilistic analyses are run using 1,000 Monte-Carlo simulations. It has been observed during this investigation that the probabilistic model representing Fruitgrowers Dam associated with 1,000 Monte-Carlo simulations returns a probability that can vary up to 3 percent as shown in figure 23.

During all probabilistic and deterministic analyses, all soil properties are considered uncorrelated among themselves.

The results of the probabilistic analyses as well as the comparison with the results generated by Slope/W version 7.14 are described in the following section.

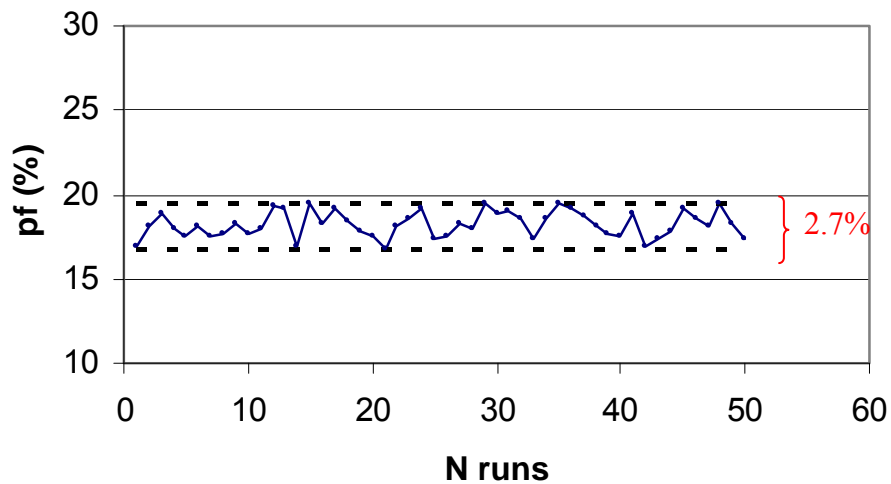


Figure 23.—Variability in *pf* results using 1,000 Monte-Carlo simulations. To recognize how much the *pf* computed by the Fruitgrowers model could vary in a probabilistic setting, the same data file was run 50 times.

**Fruitgrowers deterministic and probabilistic results comparison
between the programs *Pf-slope* and *Slope/W***

The result from the deterministic preliquefaction model run using *Pf-slope* shows FS=1.66 (figure 24) while the *Slope/W* result according to Spencer’s Method returns FS=1.746 (figure 25). The deterministic postliquefaction model computed by *Pf-slope* returned a value of FS=1.09 (figure 26) when the *Slope/W* result on the same model according to Spencer’s Method returned FS=1.06 (figure 27).

The postliquefaction analysis results from both programs assumes the presence of a liquefiable layer 54 feet long while the postliquefaction deterministic analysis computed in 2004 obtained FS=1.05 assuming the presence of a liquefiable layer 60 feet in length.

In the probabilistic analysis computed by *Pf-slope*, the same values used in the postliquefaction analysis characterize the deterministic variables, and the statistical parameters summarized in the previous section describe the probabilistic values. In the probabilistic analysis computed using *Slope/W*, the failure surface associated with the FS of 1.06 (figure 27) was chosen as the critical one to test with the probabilistic approach offered by *Slope/W*.

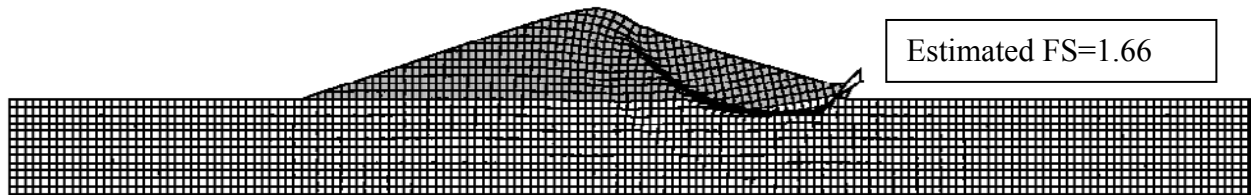


Figure 24.—DIS file showing displacement associated with the deterministic preliquefaction conditions at Fruitgrowers Dam.

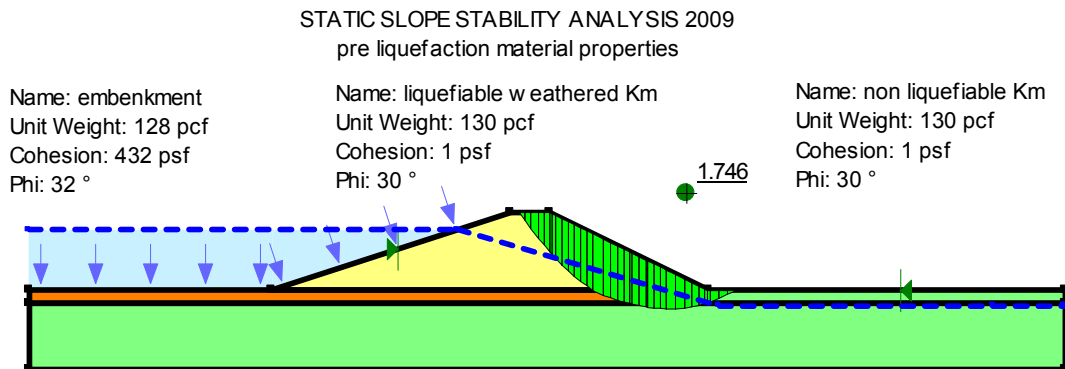


Figure 25.—Graphical representation according to Spencer’s Method of the *Slope/W* results describing the deterministic preliquefaction conditions at Fruitgrowers Dam.

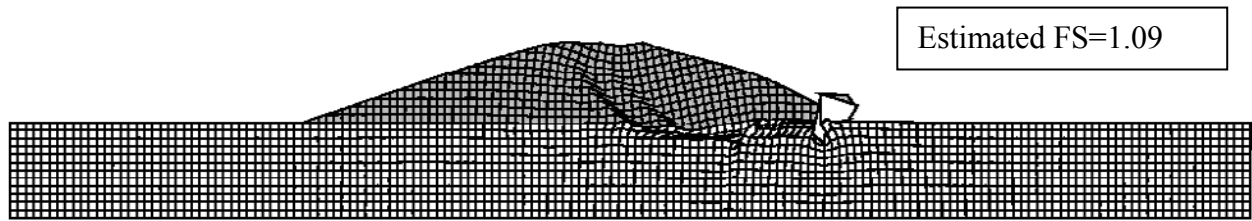


Figure 26.—.DIS file from *Pf-slope* showing displacement associated with the deterministic postliquefaction conditions at Fruitgrowers Dam.

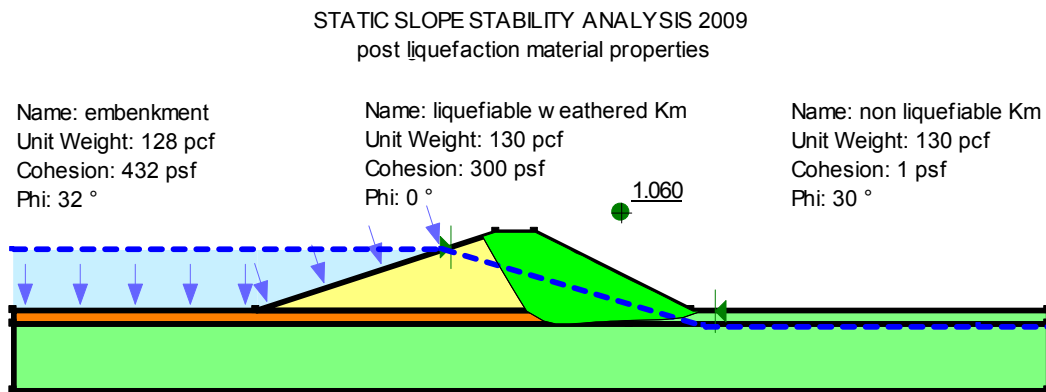


Figure 27.—Graphical representation according to Spencer's Method of the Slope/W results describing the deterministic postliquefaction conditions at Fruitgrowers Dam.

The soil property statistical parameters and soil spatial variation parameters used in this analysis are the same as those used in the analysis run with *Pf-slope* and are summarized in tables 2, 3, and 4. Tables 5 and 6, respectively, summarize the results from the Slope/W analyses and the analyses run with *Pf-slope*. Figure 28 shows a direct comparison of the results from the two programs for both lower and higher CoV .

The results shown in figure 28 outline fundamental differences between the two programs. A detailed effort has been made during this study to comprehend the differences among the two programs, but while, for *Pf-slope*, a full version of the program's code is available, for Slope/W, the author of this research has to rely solely upon the program manual, published by Geostudio, which does not provide detailed information on the program code.

The results of additional comparisons between *Pf-slope* and Slope/W, in agreement with the trend shown in figure 28, confirmed that the probability of $FS < 1$ computed by Slope/W, is in all cases, unconservative with respect to the probability estimate computed by *Pf-slope*. The main reasons explaining the difference in *pf* results and the unconservative trend shown by the Slope/W *pf* results are discussed in the following paragraphs.

Probabilistic Slope Stability Analysis Using the
Random Finite Element Method (RFEM)—Report of Findings

Table 5.—Results from the Fruitgrowers probabilistic analyses run with Slope/W

Low CoV		High CoV	
(θ) ft	<i>pf</i> %	(θ) ft	<i>pf</i> %
4	3.8	4	20.12
10	12.53	10	34.23
15	19.37	15	39.02
20	23.37	20	43.48
25	26.41	25	45.48
30	28.47	30	45.95
35	28.21	35	46.39
40	28.69	40	46.4
50	29.14	50	46.35
500	29.28	500	46.72

Table 6.—Results from the Fruitgrowers probabilistic analyses run with *Pf-slope*

Low CoV		High CoV	
(θ) ft	<i>pf</i> %	(θ) ft	<i>pf</i> %
4	94.7	4	98.6
25	72.9	25	95.8
60	70.3	60	89
100	66.7	100	82.7
200	66.4	200	78.6
300	65.9	300	77.9
500	67.3	500	73.5

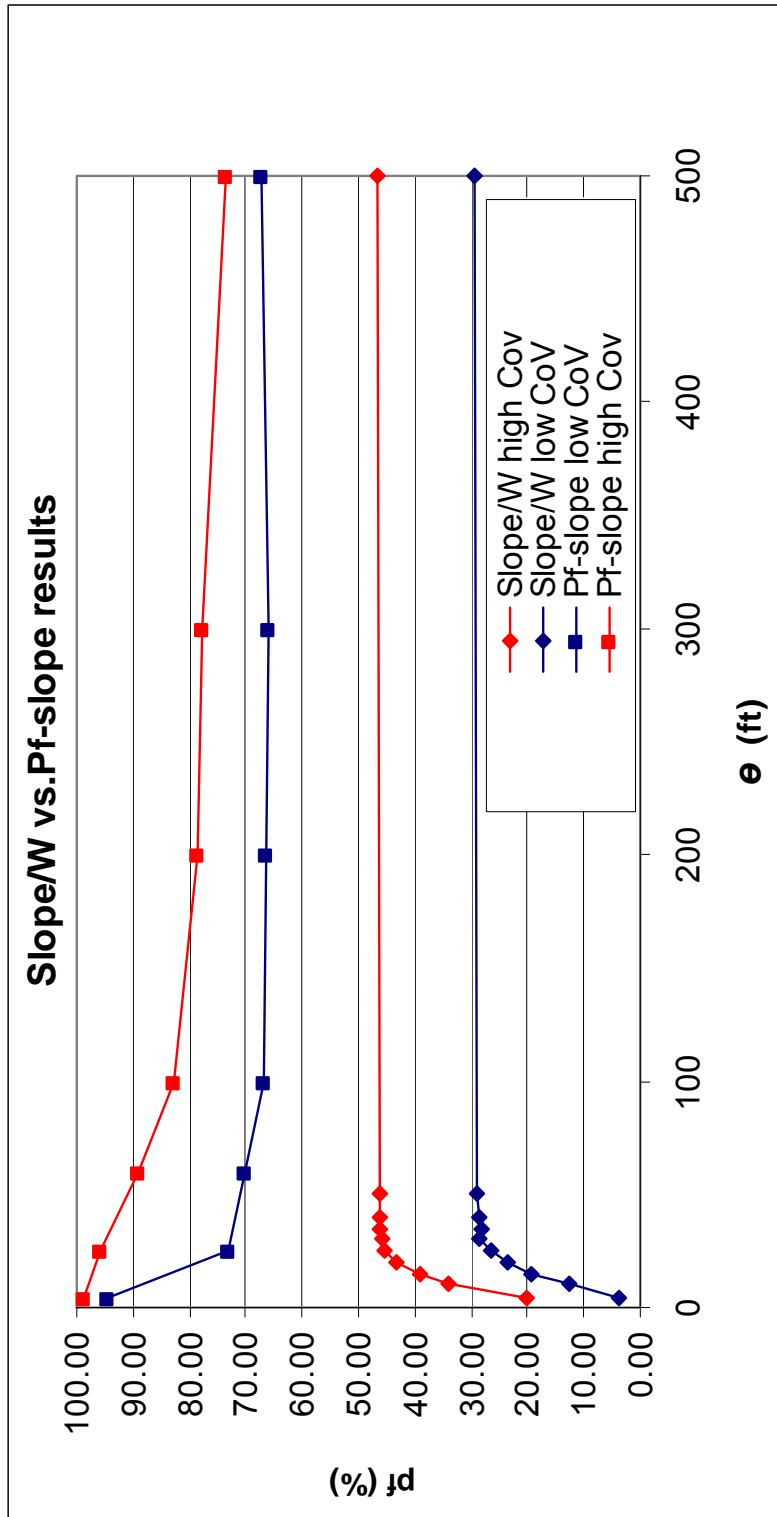


Figure 28.—Comparison of the results from programs *Pf-slope* and *Slope/W* for both lower and higher *CoV*. *Pf-slope* results are based on the deterministic FS of 1.09 the and *Slope/W* results on the deterministic FS of 1.06.

It is important to remember that for both probabilistic and deterministic analyses, the Slope/W program represents a 1-dimensional model of the soil property correlations characterizing the site while *Pf-slope* characterizes the soil property correlations using a 2-dimensional model. In the probabilistic approach, *Pf-slope* investigates the soil variability through the spatial correlation length on the entire foundation area and the entire embankment area whereas Slope/W investigates the soil variability only along the line characterizing the critical slip surface.

Another major difference between the two programs is that Slope/W computes the probabilistic analysis on a failure surface found using traditional slope stability methods (Jambu, Spencer, Bishop etc..) that do require a subdivision of the slope into columns while *Pf-slope*, based on a strength reduction technique (*SRF*), allows the modeled slope to fail without setting initial geometric constraints to the problem. In the author's opinion, the number of columns initially selected by the user influences not only the precision of the deterministic FS, but also the computation of the probability of failure. The Slope/W manual clarifies that the lower probability of failure should be associated with the option of sampling the slope at each slice, "The probability of failure is the highest when the soil is sampled only once for each trial run and is the lowest when the soil is sampled for each slice." The author conducted an analysis to better comprehend the influence of an increasing number of slices on the Slope/W *pf* computation. This analysis revealed that the *pf* of a slope with $FS > 1$, characterized by high *CoV* and spatial correlation length equal to the average width slice, can vary up to about 10 percent (if the same problem is analyzed using 60 slices compared to 15 slices). Furthermore, a sampling distance smaller than the average slice width returns an invariant *pf*. So it is the opinion of the author that when the user chooses the number of slices characterizing the slope he/she is also putting a constraint on the minimum values of spatial correlation length (or scale of fluctuation for the Slope/W program) to which Slope/W is sensitive, therefore influencing the resulting *pf*.

Another component likely responsible for the low values of probability characterizing the Slope/W curves, especially at lower values of spatial correlation length (θ), is the computation of the variance function.

Figure 28 shows that for high values of spatial correlation, the *pf* results from both programs show very little variation, which is expected because high values of spatial correlation correspond to a virtually homogeneous soil material. Lower values of spatial correlation, instead, emphasize a very different trend between the two programs.

For *Pf-slope*, high values of probability of $FS < 1$ or nonconvergence are associated with low spatial correlation values (variable soil), and a decreasing trend of *pf* can be observed with more and more homogeneous soil (high spatial correlation values). This trend is confirmed in the literature by various papers describing

probability of failure computed by finite elements and based on the strength reduction technique (e.g., Griffiths and Fenton, 2004).

For the same problem, the Slope/W trend associates lower pf with a highly variable soil (low spatial correlation) and a higher pf with a more homogeneous soil (high spatial correlation). A detailed study of this trend through questions and correspondence with the Geostudio Support Center have led the author to believe that a cause for this difference can be attributed to the way the variance function is computed. In *Pf-slope*, the function $\gamma(T)$, where (T) represents the 2-dimensional averaging domain, is called the variance function. The variance function lies between 0 and 1 and gives the amount that the variance is reduced when the covariance function $X(t)$ is averaged over the averaging domain (T) . For domain=0, the variance function has a value of 1; therefore, the variance is equal to the covariance value and is not reduced at all. Instead, as the domain becomes larger, the variance function decreases toward 0. The variance function can be expressed by the form:

$$\gamma(T) = \frac{1}{(T)^2} \int_0^T \int_0^T \rho_x(\xi - \eta) d\xi d\eta \quad (19)$$

When the correlation function ρ between properties is small (in the case of Reclamation's model, the properties are not correlated at all), the correlation function is highly reduced. On the other hand, if soil properties are perfectly correlated ($\rho=1$), the variance function equals 1, and no reduction is applied.

In Slope/W, a reduction factor is applied to the correlation function according to the theory proposed by Vanmarcke (1983) and expressed in the form:

$$\rho(\Delta Z, \Delta Z') = \frac{Z_0^2 \Gamma(Z_0) - Z_1^2 \Gamma(Z_1) + Z_2^2 \Gamma(Z_2) - Z_3^2 \Gamma(Z_3)}{2 \Delta Z \Delta Z' [\Gamma(\Delta Z) \Gamma(\Delta Z')]^{0.5}} \quad (20)$$

where,

- $\Delta Z, \Delta Z'$ = the length between two sections
- Z_0 = the distance between the two sections
- $Z_1 = \Delta Z + Z_0$
- $Z_2 = \Delta Z + Z_0 + Z'$
- $Z_3 = \Delta Z' + Z_0$ and,
- Γ = a dimensionless variance function

In equation 20, the dimensionless variance function Γ is approximated according to Vanmarcke theory (1983) by:

$$\Gamma(Z) = 1 \quad (21)$$

when the length between two sections ΔZ is equal to or less than the scale of fluctuation or spatial variation length, and

$$\Gamma(Z) = \frac{\delta}{Z} \quad (22)$$

when the length between two sections ΔZ is equal to or greater than the scale of fluctuation or spatial variation length.

In the specific case of the model representing Fruitgrowers Dam, the average distance between two slices is approximately 4 feet, and therefore, no reduction was applied to the variance function throughout all analyses. A random field characterized by a reduced mean and variance values would lead to higher probability of failure, and that could explain why the Slope/W results are consistently unconservative with respect to the results computed by *Pf-slope*. It has been tested that when the spatial correlation length value is equal to or smaller than the element size in cases where $FS > 1$ and CoV is very high (0.9), the *pf* computed by *Pf-slope* could be underestimated. This can happen because the influence of the spatial correlation length parameter in the probability computation is actually less than the influence of the local averaging. Nevertheless, this situation does not apply to the specific analysis of Fruitgrowers Dam.

And even for the cases when this may apply, one unstable result certainly cannot in any way change the overall interpretation of the analysis results trend.

Undoubtedly, it is quite difficult to determine the correct value of a soil's variability, and this parameter represents a key component of this probabilistic analysis. Only expert engineering judgment supported by exploration can truly lead to the understanding of what that meaningful range of soil variability is for a specific material. The results computed by *Pf-slope* and shown in figure 28 clearly emphasize that not accounting properly for soil variability will lead to unconservative results of probability of $FS < 1$, or nonconvergence, and underestimate the probability of slope instability.

Ridgway Dam

Ridgway Dam is located 1 mile north of Ridgway Colorado, on the Uncompahgre River at a location just above the confluence of Dallas Creek in Ouray County, Colorado. Construction of the Dam started in 1978 and was completed in 1987. Ridgway Reservoir has a capacity of 84,591 acre-feet at reservoir water surface elevation 6871.3 (top of water conservation). The dam is a compacted zoned earthfill structure that as a structural height of approximately 330 feet, a hydraulic height of approximately 206 feet, a crest width of 30 feet, and a crest length of 2,430 feet at elevation 6886 feet. The upstream face has a 3:1 (horizontal to vertical) slope from the crest down to a 20-foot wide berm at elevation 6790 and a 3.5:1 slope down to the foundation. A 3-foot thick layer of riprap protects the upstream face.

The downstream face has a 2.5:1 slope down to elevation 6800 and a 3:1 slope down to the foundation. The downstream face is characterized by selected silt, sand, gravel, and cobbles to 12-inch size and has a 6-inch thick seeded topsoil. A cut-off trench was excavated through valley surficial deposits into bedrock with a maximum depth of 115 feet and is, for the most part, located along the dam centerline.

The base of the trench at maximum section is approximately 160 feet wide with side slopes at 1.5:1. Beyond the limit of the cut-off trench, the embankment materials were placed directly on alluvial material. The general plan view and cross sections of the dam are shown in figure 29.

Ridgway Dam is located in a glacial valley close to the outwash source. The Mancos Shale Formation is found in the upper mesas, the Dakota Formation on the upper left abutment, and the Morrison Formation on the abutments and the valley. The Morrison Formation consists of sandstones, siltstones, and mudstones.

Surficial materials remaining under the dam consist primarily of Quaternary alluvium (Qal) with lesser amounts of buried Quaternary landslide deposits (Qls). The alluvium includes stream fill, low level terraces, and floodplain deposits and consists mainly of stream-deposited, rounded to well rounded gravels, cobbles, and boulders with some sand and minor amounts of silt and clay.

Figure 30 shows a geologic cross section along the maximum section of the dam. More information on the geology and engineering properties of the embankment and the foundations at the site are available in Technical Memorandum No. RD-8312-6 (Reclamation, 2003).

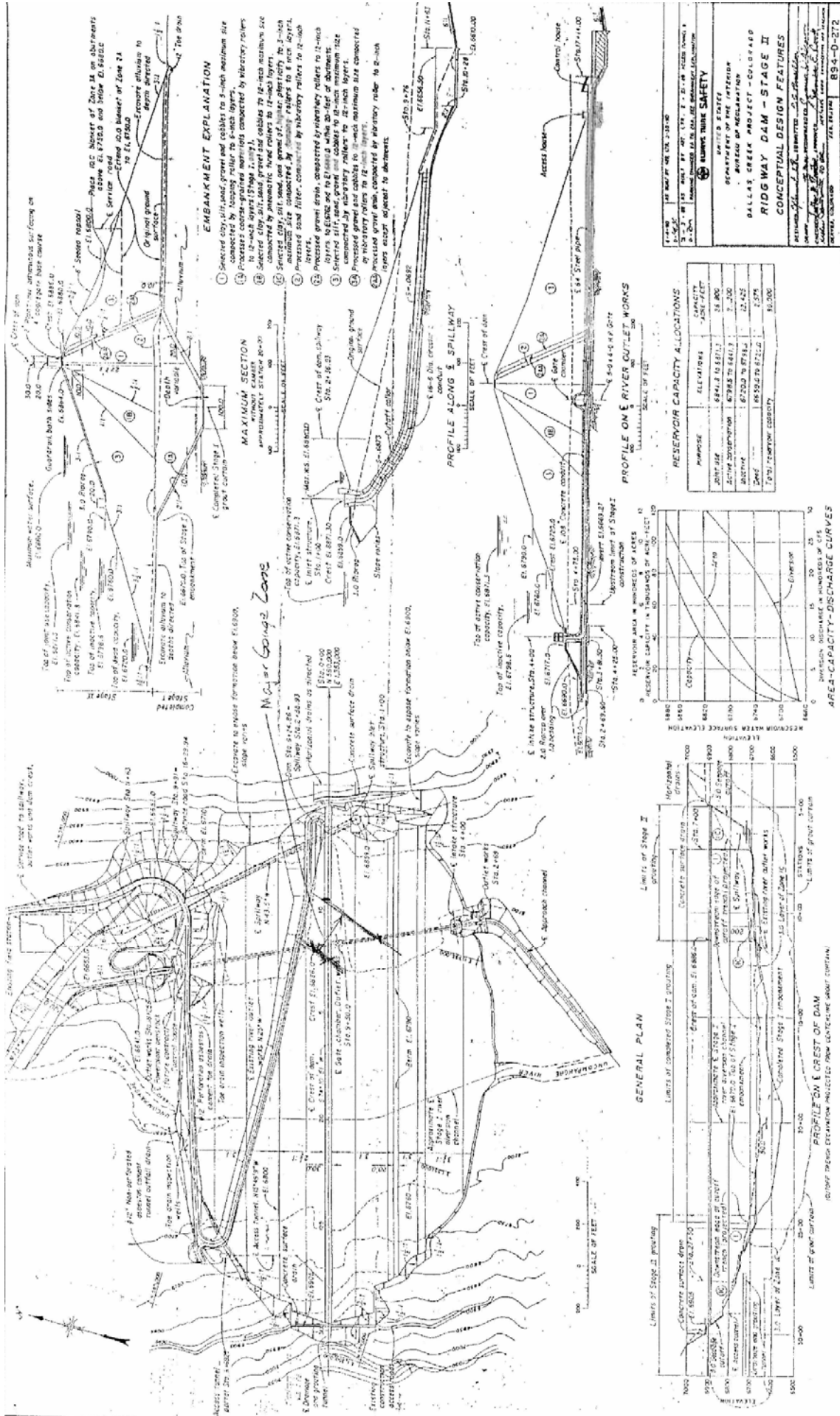


Figure 29.—General plan view and cross sections of Ridgway Dam.

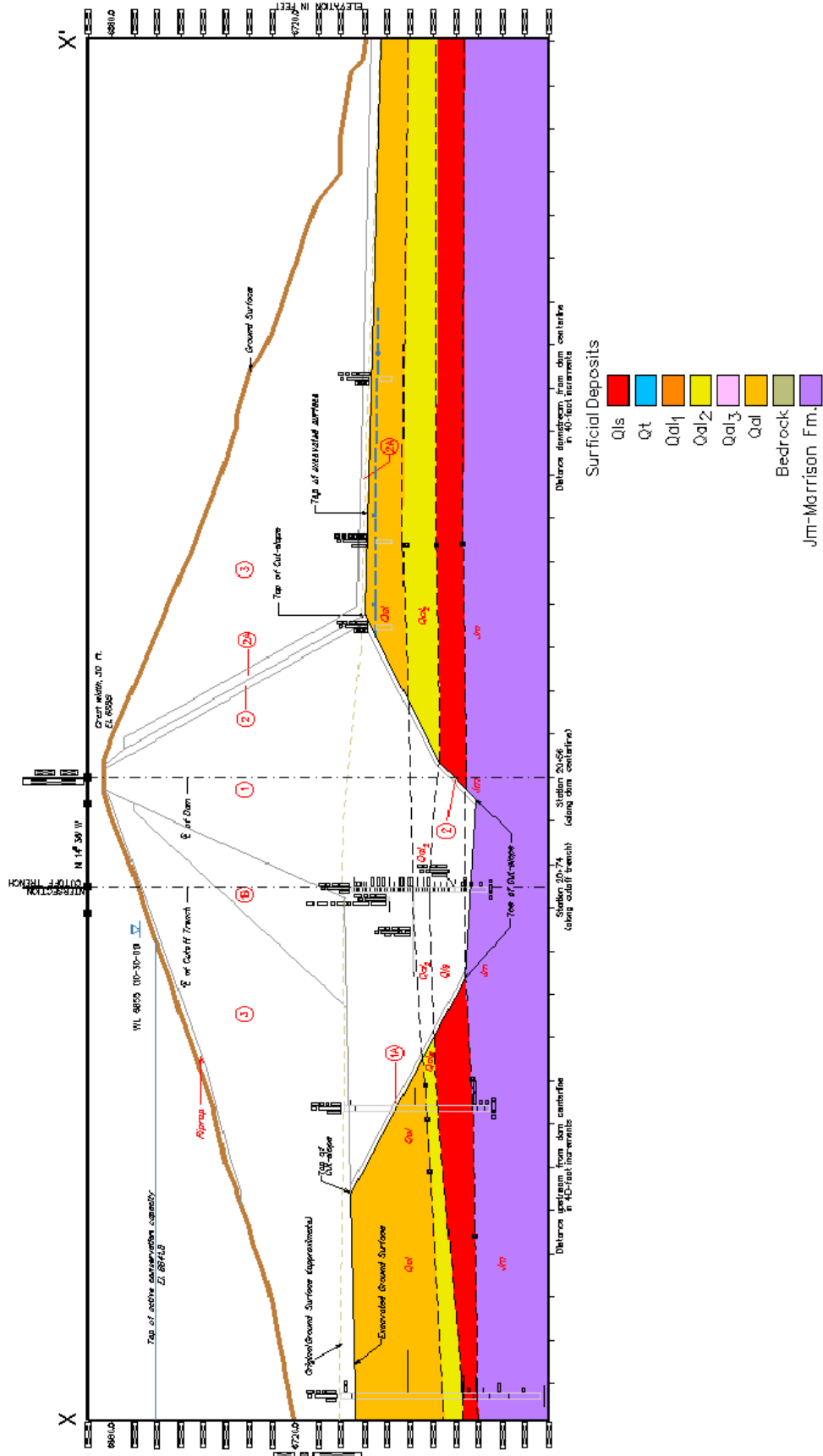


Figure 30.—Geologic cross section along the maximum section of Ridgway Dam.

Background analyses

The first dynamic analysis of Ridgway Dam was performed in 1981 and indicated that induced deformations for up to a magnitude 7.0 earthquake would not be sufficient to cause an overtopping failure of the dam. According to the 1999 Comprehensive Facility Review of the dam by Reclamation, the foundation material was considered to contain potentially liquefiable materials. Based on this observation, a slope stability assessment of the dam was conducted in 2003 to estimate the actual displacements that might occur as a result of a seismic event. The analysis conducted in 2003 indicates that there is a continuous or interconnected zone of liquefiable materials in the foundation and that a significant downstream slope failure would occur during a seismic event. It was also determined that a minimum of 350 feet to 400 feet, upstream to downstream, of liquefiable material would be required to cause a liquefaction-related failure.

The geometry and material assumptions used in the 2003 analysis were the same as those used in the 1981 dynamic analysis except that the zone 1 strength characterized by a friction angle of 25 degrees in the 2003 analysis was not reduced by 20 percent as it was in the 1981 analysis. The 2003 analysis only used failure surfaces passing through the downstream foundation because the cut-off trench beneath the dam is located upstream of the centerline and would increase the stability of failure surfaces passing through the upstream foundation. In 2008, a slope stability analysis by Reclamation modeling possible postliquefaction conditions showed FS=1.09 (figure 31). This analysis was conducted using the software Slope/W version 7.11 using Spencer's Method. The soil properties used in the 2008 postliquefaction study were the same as those used in the 1981 dynamic analysis. In spring 2009, Reclamation contracted with the civil engineering firm URS to review the results from site investigations performed by Reclamation in recent years and develop recommended strengths to be used in a new dynamic deformation analysis.

Current analyses

While the overall dimensions of the Ridgway Dam model in the current analyses are the same as those used in the 2008 slope stability analysis, the model has been simplified. To simplify the computational aspect of *Pf-slope*, the filters have been removed from the embankment structures. The cut-off trench has also been removed because the failure surfaces in the 2008 slope stability analysis appear to be independent from the cut-off trench. Even though the filters have been removed, the phreatic surface in the model is the same as the one used in the 2008 analysis and represents the top of active conservation capacity at 6871 feet, 15 feet below the crest. This assumption was made in an attempt to model a condition more similar to what the site is experiencing. Generally, the model portrays an embankment section characterized by a core material (zone 1) and a shell material (zone 2) placed in the upstream and downstream outer embankment sections. The foundation section is characterized by a homogeneous alluvium material approximately 100 feet thick, and a potentially liquefiable layer, located under the downstream side of the dam about 20 feet below the surface. The

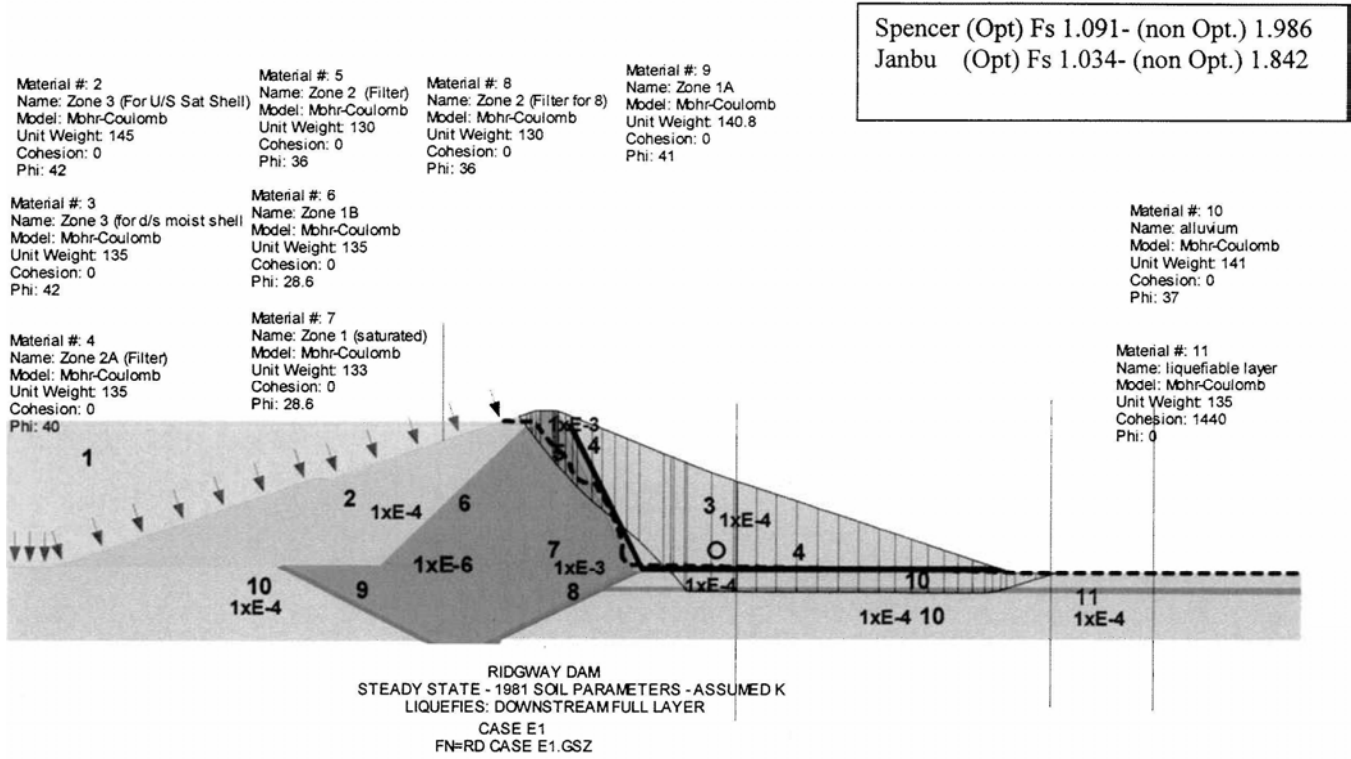


Figure 31.—Representation of the 2008 model used in the deterministic postliquefaction analysis.

liquefiable layer is assumed to be about 5 feet thick, and 1,010 feet in length from the location where it would theoretically intercept the cut-off trench to the right boundary of the model.

Similarly to the approach used for the analysis performed on Fruitgrowers Dam, deterministic pre- and postliquefaction analyses were conducted for the Ridgway Dam case history. The soil properties used in the deterministic analyses to characterize the embankment zones, foundation, and liquefiable layer in the foundation were taken from the URS study conducted in spring 2009 and are summarized in table 7.

The results from these deterministic analyses as well as the comparison with the results generated by Slope/W version 7.14 used by Reclamation are described in the next section, *Ridgway deterministic and probabilistic results comparison between Pf-slope and Slope/W*.

Following the same approach used for the previous case history, the postliquefaction deterministic model is run using the probabilistic capability offered by *Pf-slope*. The soil properties as probabilistic variables and their statistical parameters used during the probabilistic analysis are summarized in table 8.

Probabilistic Slope Stability Analysis Using the
Random Finite Element Method (RFEM)—Report of Findings

Table 7.—Deterministic soil properties used in Ridgway Dam pre- and postliquefaction analyses

Liquefaction condition	Material	Unit weight (lb/ft ³)	ϕ' (°)	c' (lb/ft ²)
Postliquefaction	Embankment core	133	28.6	1
	Embankment shell	138	42	1
	Foundation	141	37	1
	Quaternary alluvium	135	5	1440
Preliquefaction	Embankment core	133	28.6	1
	Embankment shell	138	42	1
	Foundation	141	37	1
	Quaternary alluvium	Layer removed in the preliquefaction analysis		

Table 8.—Probabilistic soil properties used in Ridgway postliquefaction analyses

Material	Mean	Standard deviation, lower CoV	Standard deviation, higher CoV	Distribution type
Embankment core ϕ (°)	28.6	NA	NA	deterministic
Embankment core cohesion (lb/ft ²)	1	NA	NA	deterministic
Embankment shell ϕ (°)	42	6.3	25.2	lognormal
Embankment shell cohesion (lb/ft ²)	1	0.15	0.6	lognormal
Foundation ϕ (°)	37	11.1	22.2	lognormal
Foundation cohesion (lb/ft ²)	1	0.3	0.6	lognormal
Quaternary alluvium ϕ (°)	5	1.5	3.0	lognormal
Quaternary alluvium cohesion (lb/ft ²)	1,440	432	864	lognormal

Similarly to the approach used for the Fruitgrowers analysis, the Ridgway probabilistic analysis associates one random field with the embankment and one with the foundation, and the liquefiable layer is described by the foundation random field, which is modified to address the new values describing the liquefiable material. Because the core material can be considered an engineered material with very little variability, for simplicity, this analysis considered the core area using deterministic soil properties.

In this probabilistic model, only the strength parameters of friction and cohesion are analyzed with a probabilistic approach; the other parameters, dilation angle, unit weight, Young's modulus, and Poisson's ratio are analyzed following a deterministic approach.

To address the level of uncertainty incorporated into the mean values describing the properties, the same probabilistic model is run one time with a higher *CoV* and one time with a lower *CoV*. The *CoV* values used in each analysis for all material types are summarized in table 9

Table 9.—*CoV* values characterizing Ridgway probabilistic runs

Material	Lower <i>CoV</i>	Higher <i>CoV</i>
Embankment shell ϕ (°) and cohesion (lb/ft ²)	0.15	0.3
Foundation ϕ (°) and cohesion (lb/ft ²)	0.3	0.6
Quaternary alluvium ϕ (°) and cohesion (lb/ft ²)	0.3	0.6

Also, for the Ridgway Dam probabilistic analysis, the *CoV* values were chosen by evaluating suggested values available in the literature for similar soil material (e.g., Phoon and Kulhawy, 1999).

The set of isotropic values chosen to investigate the spatial correlation length θ for all Ridgway probabilistic runs is reported in table 10.

Table 10.—Isotropic θ values (ft) characterizing Ridgway spatial variation of soil

4
25
60
100
200
300
500
2,000

All the probabilistic analyses were run using 1,000 Monte-Carlo simulations. Applying the same methodology adopted for Fruitgrowers Dam, it has been observed during this investigation that the probabilistic model created to represent Ridgway Dam associated with 1,000 Monte-Carlo simulations returns a probability that could vary up to 3 percent.

During all probabilistic and deterministic analyses, all soil properties are considered uncorrelated between each other.

In the following section, the results of the probabilistic analyses as well as the comparison with the results generated by Slope/W are described.

Ridgway deterministic and probabilistic results comparison between *Pf-slope* and Slope/W

The result from the deterministic preliquefaction model run using *Pf-slope* shows FS=2.31 (figure 32) while the Slope/W result according to Spencer’s Method returns FS=2.49 (figure 33).

The deterministic postliquefaction model was initially run entirely frictionless with a liquefiable layer, and this assumption, as shown in figures 34 and 35, led to very low FS for both programs (*Pf-slope* FS=0.58, Slope/W FS=0.6). Since it would not be very meaningful to run the probabilistic approach with such low FS, a second deterministic postliquefaction analysis was run with a liquefiable layer characterized by a friction angle equal to 5 degrees.

This second analysis computed by *Pf-slope* returned a value of FS=0.97 (figure 36) while the Slope/W result on the same model according to Spencer’s Method returned FS=1.07 (figure 37).

In the probabilistic analysis computed by *Pf-slope*, the same values used in the postliquefaction deterministic analysis characterize the deterministic variables, and the statistical parameters summarized in the previous section describe the probabilistic values.

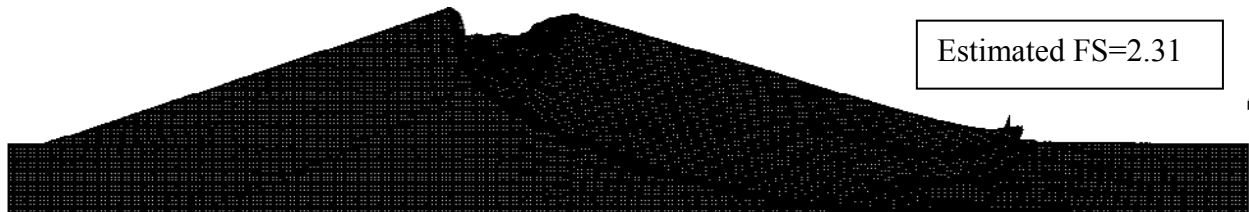


Figure 32.—DIS file showing displacement associated with deterministic preliquefaction conditions at Ridgway Dam.

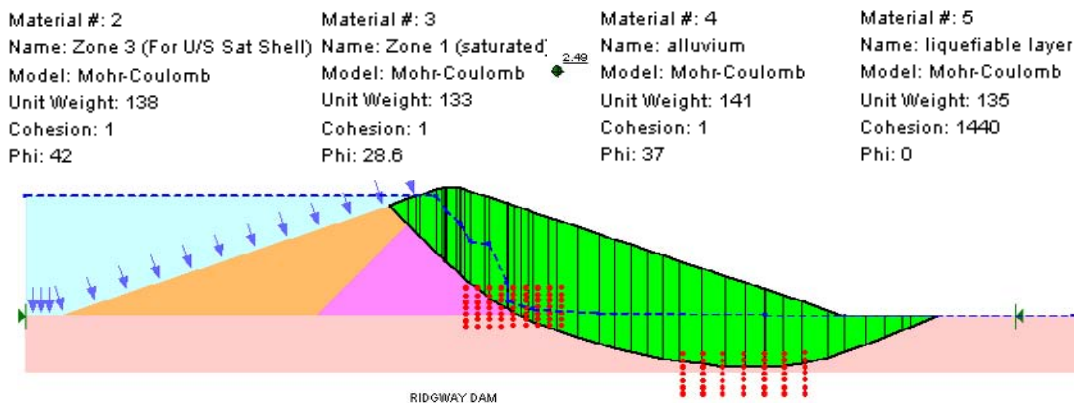


Figure 33.—Graphical representation according to Spencer’s Method of the Slope/W results describing deterministic preliquefaction conditions at Ridgway Dam.

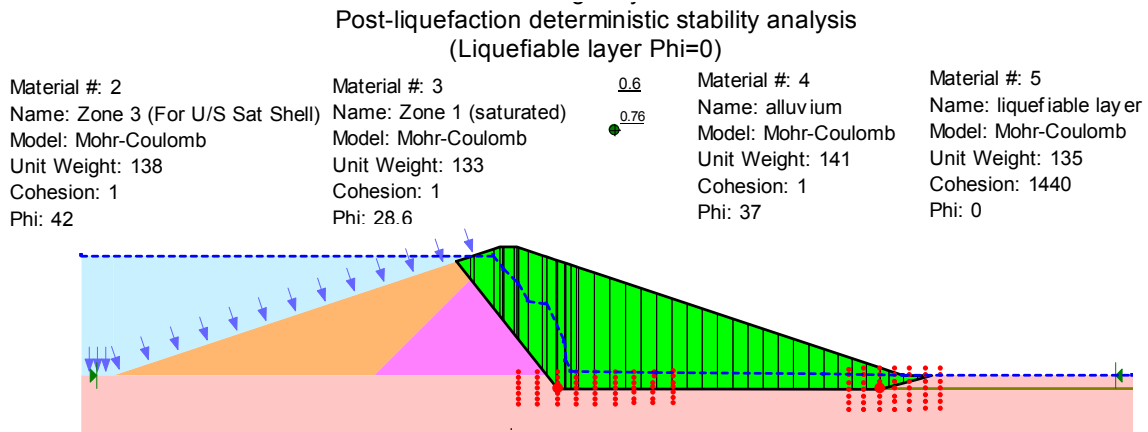


Figure 34.—Graphical representation according to Spencer’s Method of the Slope/W results describing the deterministic postliquefaction conditions at Ridgway Dam when the liquefiable layer is assumed to be frictionless.



Figure 35.—DIS file showing displacement associated with the deterministic postliquefaction conditions at Ridgway Dam when the liquefiable layer is assumed to be frictionless.

For the Ridgway probabilistic analysis computed using Slope/W, the failure surface associated with an FS of 1.07 (figure 37) was chosen as critical to test with the probabilistic approach offered by Slope/W. The soil properties statistical parameters and soil spatial variation parameters used in this analysis are the same as those used in the analysis run with *Pf-slope* and are summarized in tables 8, 9, and 10.

Tables 11 and 12 summarize the results for the Ridgway case history from the analyses run with Slope/W and *Pf-slope*, respectively. Figure 38 shows a direct comparison of the results from the two programs for both lower and higher *CoV*.

The results shown in figure 38, computed by *Pf-slope* and Slope/W for the Ridgway Dam model, confirm the trend of the results of the previous case history of Fruitgrowers Dam. While both programs show very little variation in *pf* with high values of spatial correlation, which is expected because high values of spatial correlation correspond to a virtually homogeneous soil material of each simulation, for lower values of spatial correlation length, the results given by Slope/W for each analysis are unconservative with respect to the results produced by *Pf-slope*.

Probabilistic Slope Stability Analysis Using the
Random Finite Element Method (RFEM)—Report of Findings

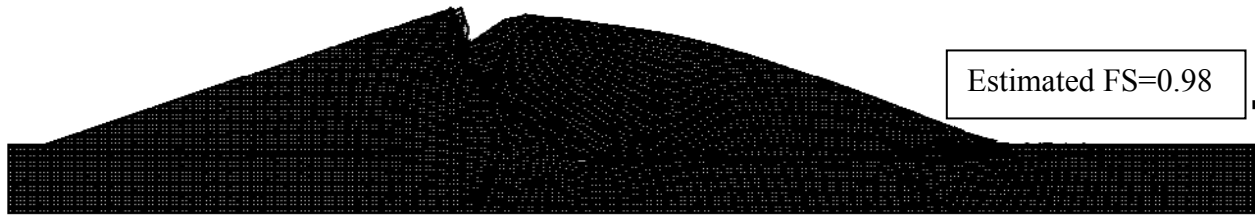


Figure 36.—DIS file showing displacement associated with deterministic postliquefaction conditions at Ridgway Dam when a friction angle of 5° characterizes the liquefiable layer.

Material #: 2	Material #: 3	Material #: 4	Material #: 5
Name: Zone 3 (For U/S Sat Shell)	Name: Zone 1 (saturated)	Name: alluvium	Name: liquefiable layer
Model: Mohr-Coulomb	Model: Mohr-Coulomb	Model: Mohr-Coulomb	Model: Mohr-Coulomb
Unit Weight: 138	Unit Weight: 133	Unit Weight: 141	Unit Weight: 135
Cohesion: 1	Cohesion: 1	Cohesion: 1	Cohesion: 1440
Phi: 42	Phi: 28.6	Phi: 37	Phi: 5

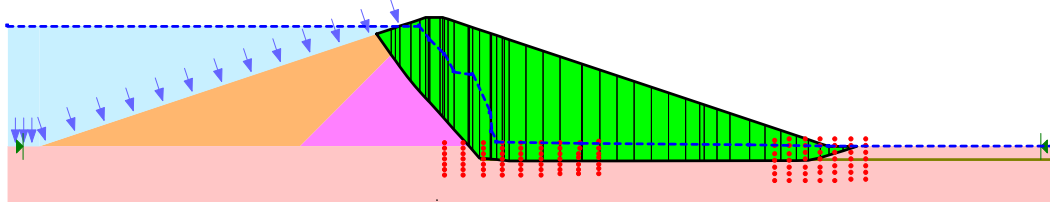


Figure 37.—Graphical representation according to Spencer's Method of the Slope/W results describing deterministic postliquefaction conditions at Ridgway Dam when a friction angle of 5° characterizes the liquefiable layer.

The same reasons discussed for the of results associated with the Fruitgrowers analysis in an attempt to explain the different trends given by the two programs apply to the probabilistic analysis for Ridgway Dam. In accordance with the results from the Fruitgrowers Dam analysis, the probabilistic analysis for Ridgway Dam clearly emphasizes that underestimating the influence of soil variability in computations of probability of failure will lead to unconservative results of probability and underestimate the risk of slope instability.

Table 11.—Results from the Ridgway probabilistic analyses run with Slope/W

Low CoV		High CoV	
(θ) ft	<i>pf</i> %	(θ) ft	<i>pf</i> %
4	2.71	4	16.45
10	2.41	10	16.76
15	2.34	15	16.16
20	2.6	20	16.37
25	3.27	25	18.43
30	5.26	30	20.16
35	5.16	35	20.7
40	4.75	40	20.18
50	6.27	50	24.08
100	12.76	100	31.11
200	18.91	200	36.53
350	26.93	350	42.45
500	29.81	500	43.74
600	29.96	600	43.87
800	30.78	800	43.94
1,000	30.94	1,000	43.95
2,000	31.75	2,000	45.82

Table 12.—Results from the Ridgway probabilistic analyses run with *Pf-slope*

Low CoV		High CoV	
(θ) ft	<i>pf</i> %	(θ) ft	<i>pf</i> %
4	99.9	4	100
25	96	25	100
60	92	60	100
100	89.6	100	100
200	80.9	200	100
300	78.5	300	99.6
500	74.1	500	98.1

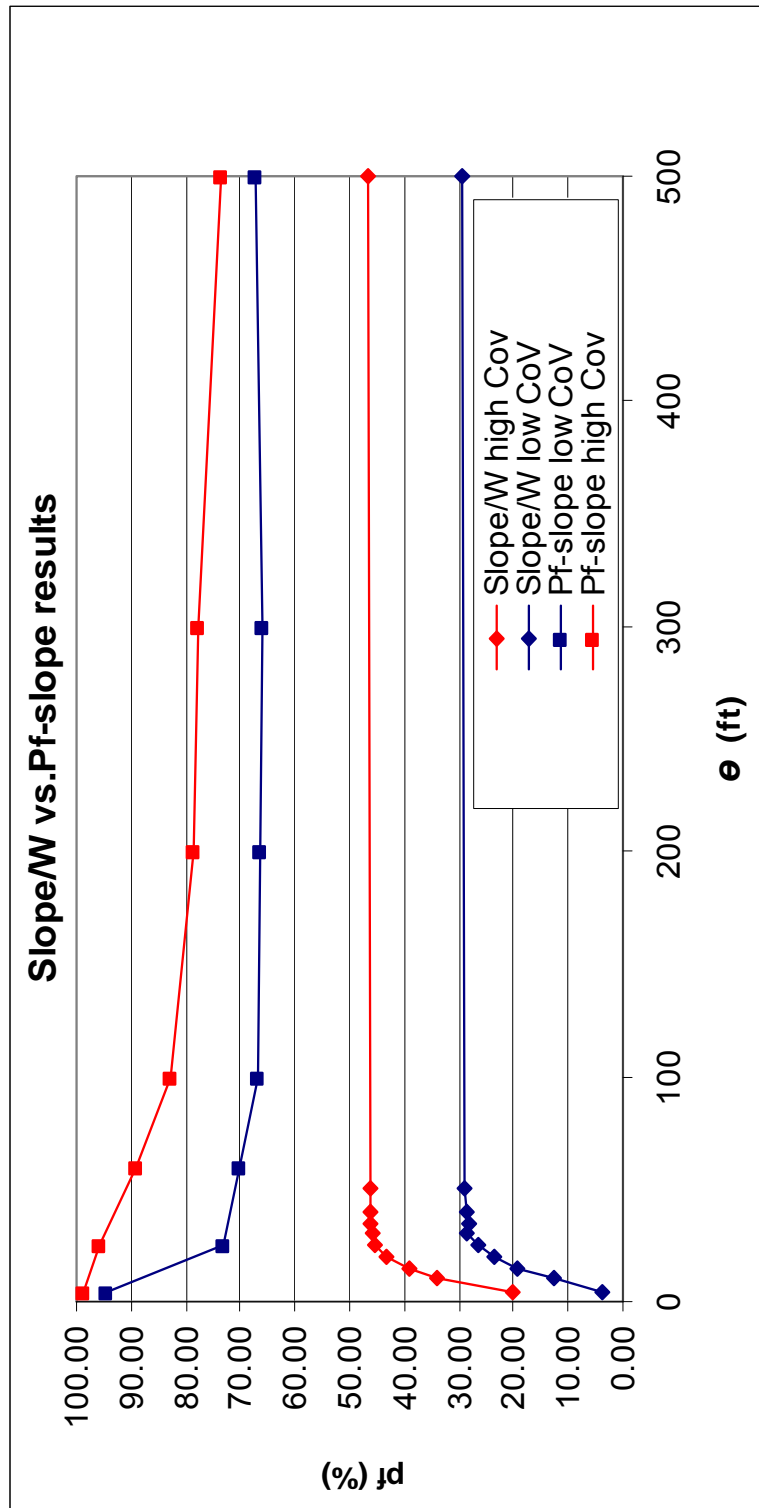


Figure 38.—Comparison of the results from *Pf-slope* and *Slope/W* for both lower and higher *CoV*. *Pf-slope* results are based on the deterministic FS of 0.98 the and *Slope/W* results on the deterministic FS of 1.07.

Conclusions

Computer program *Pf-slope*, coded in FORTRAN.95 for this research, provides a repeatable methodology capable of reducing the uncertainty of the probability of slope instability, which is a key component of an engineering structure risk assessment.

A finite element analysis of embankment structures was developed. Compared to the probabilistic approach of computer program Slope/W version 7.14, *Pf-slope* can predict the probability of $FS < 1$, or nonconvergence, in a nonhomogeneous soil structure characterized by phreatic conditions and a possible liquefiable layer. In the two case histories considered in this report, Slope/W gave consistently lower *pf* prediction than *Pf-slope*. The following three observations summarize this difference in results between the two programs:

- Slope/W program represents a 1-dimensional model, along the potential deterministic failure surface, of soil properties characterizing the site while *Pf-slope* characterizes the soil properties using a 2-dimensional random field model.
- Slope/W computes the probabilistic analysis on a failure surface found using traditional methods (Jambu, Spencer, Bishop, etc.) that do require a subdivision of the slope in columns while *Pf-slope*, based on a strength reduction technique (*SRF*) allows the slope to fail without any *a priori* assumptions about the location or shape of the failure surface.
- Different approaches to computing variance function reduction are evident between the two programs.

Furthermore, the approach used by *Pf-slope*, in contrast with any classic slope stability probabilistic methodology, accounts for soil spatial variability and can seek out the critical failure surface without assigning a predefined failure surface geometry.

The robust methodology provided by this research will not only allow testing of the stability of dams during modification phases, but will also help estimate the probability of failure in cases involving postearthquake liquefaction.

Suggestions for Future Development

The author suggests further investigations for a broader use of *Pf-slope*:

- Add capability to model a cut-off trench or buttress geometry.
- Add capability for more random soil fields in the dam embankment and the foundation.
- Study the probability of a slip surface forming in a specific location of the mesh.

The third suggestion would allow the user to understand if a critical failure surface could still retain the reservoir body based on a specific location in the mesh.

References

Borja, R.I. and S.R. Lee, “Cam-clay plasticity, Part I: Implicit integration of elasto-plastic constitutive relations,,” *Comput. Methods Appl. Mech. Engrg.* 78 (1990), pp. 49–72.

Bureau of Reclamation, *Comprehensive Facility Review Report of Findings, Dallas Creek Project, Colorado, Ridgway Dam*, by John Cyganiewicz, Bureau of Reclamation, Denver, Colorado, April 1999.

Bureau of Reclamation, Technical Memorandum No. RD-8312-6, Technical Service Center, Denver, Colorado, August 2003.

Bureau of Reclamation, *Dynamic analysis of Ridgway Dam*, Technical Memorandum No. V11-222, Division of Design, Denver, Colorado, May 15, 1981.

Bureau of Reclamation, *Ridgway Dam Dynamic Analysis*, Technical Memorandum No RD-8311-4, Geotechnical Group, Denver, Colorado, August 2003.

Bureau of Reclamation, *Fruitgrowers Dam Issue Evaluation: Evaluation of Response of Fruitgrowers Dam to Artesian Pressures in the Foundation*, Technical Memorandum No. FW-8312-2, Technical Service Center, Denver, Colorado, August 2004.

- Bureau of Reclamation, *Fruitgrowers Dam Issue Evaluation: Evaluation of Liquefaction and Post-Earthquake Stability*, Technical Memorandum No. FW8312-3, Technical Service Center, Denver, Colorado, August 2004.
- Bureau of Reclamation, *Internal documentation: Simplified Seed Analysis and Embankment Deformations*, by P.J.H., December 5, 1980.
- Bureau of Reclamation, *Comprehensive Facility Review, Report of Findings, Fruit growers Dam, Fruitgrowers Project, Colorado*, Technical Service Center, Denver, Colorado, October 1998.
- Fenton, G.A. and D.V. Griffiths, *Risk Assessment in Geotechnical Engineering*, Wiley and Sons, New Jersey, 2008.
- Fenton, G.A. and E.H. Vanmarcke, "Simulation of random fields via local average subdivision," *Journal of Eng Mech*, ASCE, 116(8):1733–1749, 1990.
- Geostudio Group, "SLOPE/W 7.14, software for Slope Stability Analysis," *Geo-SLOPE International*, 2007.
- Griffiths, D.V. and G.A. Fenton, *Probabilistic Methods in Geotechnical Engineering*, Springer Wien New York, 2008.
- Griffiths, D.V. and G.A. Fenton, "Probabilistic slope stability analysis by finite elements," *Journal of Geotechnical and Geoenvironmental Engineering ASCE*, 130(5), 507-518, 2004.
- Griffiths, D.V. and P.A. Lane, "Slope stability analysis by finite elements," *Geotechnique*, Vol. 49, No. 3, 1999, pp. 387-403.
- Griffiths, D.V., "Computation of bearing capacity factors using finite elements," *Geotechnique*, Vol. 32, No.3, pp. 195-202, 1982.
- Hicks, M.A. and R. Boughrarou, "Finite Element analysis of the Nelerk underwater berm failures," *Geotechnique*, 48(2):169-185, 1998.
- Lambe, T.W. and R.V. Whitman, *Soil Mechanics*, John Wiley and Sons, Chichester, New York, 1969.
- Matsui, T. and K-C. San, "Finite element slope stability analysis by shear strength reduction technique," *Soils and Foundations*, Vol. 32, No. 1, 1992, pp. 59-70.
- Phoon, K.K. and F.H. Kulhawy, "Characterization of geotechnical variability," *Canadian Geotechnical Journal* 36, 1999, pp. 612-624.
- Smith, I.M. and D.V. Griffiths, *Programming the Finite Element Method*, Wiley and Sons, West Sussex, England, 4th edition, 2004.

Probabilistic Slope Stability Analysis Using the
Random Finite Element Method (RFEM)—Report of Findings

Smith, I.M. and D.V. Griffiths, *Programming the Finite Element Method*, John Wiley and Sons, Chichester, New York, 3rd edition, 1998.

Smith, I.M. and D.V. Griffiths, *Programming the Finite Element Method*, John Wiley and Sons, Chichester, New York, 2nd edition, 1988.

URS Corporation, *Ridgway Dam Deformation Analysis*, Denver, Colorado, May 2009.

Vanmarcke, E.H., “Random fields: Analysis and synthesis,” The MIT Press, Cambridge, Mass., Monot, Technical report, Delft, *Geotechnics*, 1981.

**Appendix—A CD for computer program
Pf-slope, executable file**

**Including input data files for Fruitgrowers and
Ridgway Dams**